

# Reviewing the Influence of Various Nano Binders and Sintering Additives on Performance of High-Alumina Nano-Bonded Refractory Castable.

Durgesh Rai & Manas Ranjan Majhi\*

JRF, Department of Ceramic Engineering, Indian Institute of Technology (BHU), Varanasi, India

Professor, Department of Ceramic Engineering, Indian Institute of Technology (BHU), Varanasi, India

DOI: <https://doi.org/10.51583/IJLTEMAS.2026.1502000043>

Received: 13 February 2026; Accepted: 18 February 2026; Published: 09 March 2026

## ABSTRACT

The petrochemical industries have recently given refractory castable improved with nano bonding a lot of attention. The properties of the castable material have been improved by the use of different binders and sintering additives. Numerous research projects are now looking at use of different nano binders, such colloidal alumina and silica in conjunction with sintering additives like those based on aluminium or boron. The objective is to reduce energy use and enhance densification. In order to improve both thermal and mechanical characteristics, nano-structured binders in particular colloidal silica are also being investigated with a variety of raw materials, including fused silica, tabular alumina and mullite. The green strength of these nano-bonded castables is further increased by the use of setting or gelling chemicals. This review focuses on the potential of setting agents like HA and CAC, sintering additives (primarily boron-based), and nanostructured binders like colloidal silica and colloidal alumina in high alumina refractory castables intended for use in petrochemical industries, particularly FCC units.

**Keywords:** Petrochemical, Green strength, Nano bonded, Castables, Sintering Additives.

## INTRODUCTION

The study of ceramics at nanoscale, which is generally less than 100 nanometers in size, is known as nanotechnology. Ceramic nanoparticles are beneficial in a variety of applications due to their special characteristics [1]. The stability and properties of ceramic nanoparticles can withstand harsh environments, making them ideal for high-temperature applications such catalysis, fuel cells, and thermal barrier coatings [2]. In nanotechnology, materials and structures are modified and engineered at nanoscale, often on order of nanometers. The creation of binders is one of the many uses for nanomaterials and nanoparticles which also have special features and useful qualities [3]. Binders are compounds used in manufacturing, building, and other industrial operations to keep other materials together. They are employed to give materials cohesiveness and strength, such as when making adhesives, concrete, composites, or coatings. A nano binder is a type of binder that uses nanomaterials to improve its performance or qualities [4] [5]. Recent years have resulted in improved performance from refractory goods, which has been linked to continuous improvement of raw ingredients, dispersion agents, operating protocols, and construction processes [6]. However, widely accessible commercial refractory materials are still scarce for some applications such as fluid catalytic cracking units in petrochemical sector that function at temperatures below 900 °C [7]. The most often utilized binder in traditional refractory compositions used in steel-making activities is calcium aluminate cement. When this additive reacts with water, it creates hydraulic bonding between the coarse aggregates and fine matrix at ambient temperature [8].

The conversion of heavy hydrocarbon molecules into lighter ones is accomplished using a technique called fluid catalytic cracking (FCC) [9]. The three-step process of fluid catalytic cracking, which entails reaction, product separation, and regeneration, continues to be a crucial component in many refineries [10]. This repeating procedure produces lighter, higher-value products from fuel oils from vacuum distillation towers or residue from environmental evaporation stacks. The main component of petrol pool, cracked naphtha is one of the most

sought-after items [11]. The advancement of refractory materials has been fueled by nanotechnology, which offers the possibility of exact control at the nanoscale [12]. The use of nano binders and sintering additives in particular has opened up a viable path for improving the characteristics of high-alumina castables. In industries that are characterized by intense heat, hostile chemical conditions, and grueling mechanical pressures, refractory materials are essential. The structural integrity of industrial machinery including kilns, furnaces, and reactors has long been maintained with the help of high-alumina refractories, which have long been recognized as a cornerstone in this field [13]. High-Alumina Nano-Bonded Refractory Castable are a ground-breaking breakthrough as a result of the unrelenting search for better refractory materials. The performance and lifespan of refractory linings in high-temperature applications might be improved with the help of these cutting-edge materials [14].

The creation of refractory castable with higher thermo-mechanical characteristics at lower temperatures below 900 °C is facilitated by the large surface area and reactivity of nanoparticles of binder (colloidal alumina or colloidal silica) [15] [16]. Furthermore, adding an aluminium or boron-based sintering additive improves mechanical characteristics of refractory system substantially at temperatures between 500 and 1000 degrees Celsius [17] [18]. When it forms in microstructure of composition containing boron at 450 °C, transitory liquid speeds up densification by reacting with other materials in refractory mixture to create another solid borate component and enhance refractory properties. [19] [20].

This review aims to carefully explore an effects of various sintering additives and nano binders on efficiency of high-alumina nanoscale-bonded refractory castables. This review paper sets out on a thorough trip to clarify the significant effects of different nano binders and sintering additives on functionality of Nano-Bonded Refractory Castables with High-Alumina. It explores a complex world of nanomaterials and their interactions with refractory matrices, offering insight on how these developments are changing the environment of high-temperature materials. This paper gives a complete grasp of the promise and difficulties connected with these cutting-edge materials by exploring the most recent research findings, case studies, and practical applications.

### Objectives of research

- It is recommended to review and synthesize the present state of data on the use of nanobinders and sintering agents in high-alumina nano-bonded refractory castables.
- Analyze possible interactions and synergistic effects of nano binders and sintering additives in improving castable characteristics.
- Examine the impact of various sintering additives and nano binders on critical performance factors such as strength, microstructural characteristics, and resistance to abrasion and heat shock.
- Identify and assess elements such as the sorts of nano binders and sintering additives used, which influence the performance of high-alumina castables.
- Discuss the difficulties and restrictions associated with using these materials and offer potential areas for further study and improvement.

This article discusses about various types of nano binders in section 2, Nano binders influenced on refractory castables are covered in section 3. The next part includes high alumina nano bonded materials used in refractory castables.

Section 5 of this review article contains various sintering additive materials used for castables. The combination of additive and nano binders is covered in section 6. The various testing methods involved in refractory castable materials are discussed in section 7 of this article. Research gaps and challenges of all above mentioned topics are also discussed in this paper.

### Types on Nano Binders

Nanomaterials may be applied in a multitude of ways and take many different shapes. Typical forms of some common nanoparticles are discussed below:

## Nano Alumina

(Younus *et al.*, 2023) assessed the effects of Nano Alumina (NA) in two distinct fresh and hardened phases following ambient environment curing on fly ash and slag Alkalibased Activated Self Compacting Concrete (A-ASCC). As partial binder alternatives, four nano-alumina ratios (0%, 0.5%, 1%, and 1.5%) were employed [21]. (Su *et al.*, 2020) examined the implications that various NA offers on degradation obstruction, mechanical features, and structure of WC8Co cemented carbide during Spark Plasma Sintering (SPS). The results imply that the decomposition of NA in Co phase essentially enables a larger amount of FCC-Co to be present on surface of WC-Co bonded cement [22]. (Shao *et al.*, 2019) examined a mixture with 5% NA to understand how it affects Portland cement's durability. After 7 days, there is a clear rise in monosulfate level due to the incorporation of nano-alumina [23]. (Mohseniet *al.*, 2019) evaluated the structural and mechanical characteristics of lightweight geopolymer concretes reinforced with polypropylene fibers. The findings revealed that whereas adding PP fibers significantly enhanced the mechanical properties, particularly flexural strength. To determine the form of the RHA and NA particles, scanning electron micrographs, or SEM, are used. Figure 1 makes evident the spherical and irregular shapes of the NA and RHA particles, respectively [24].

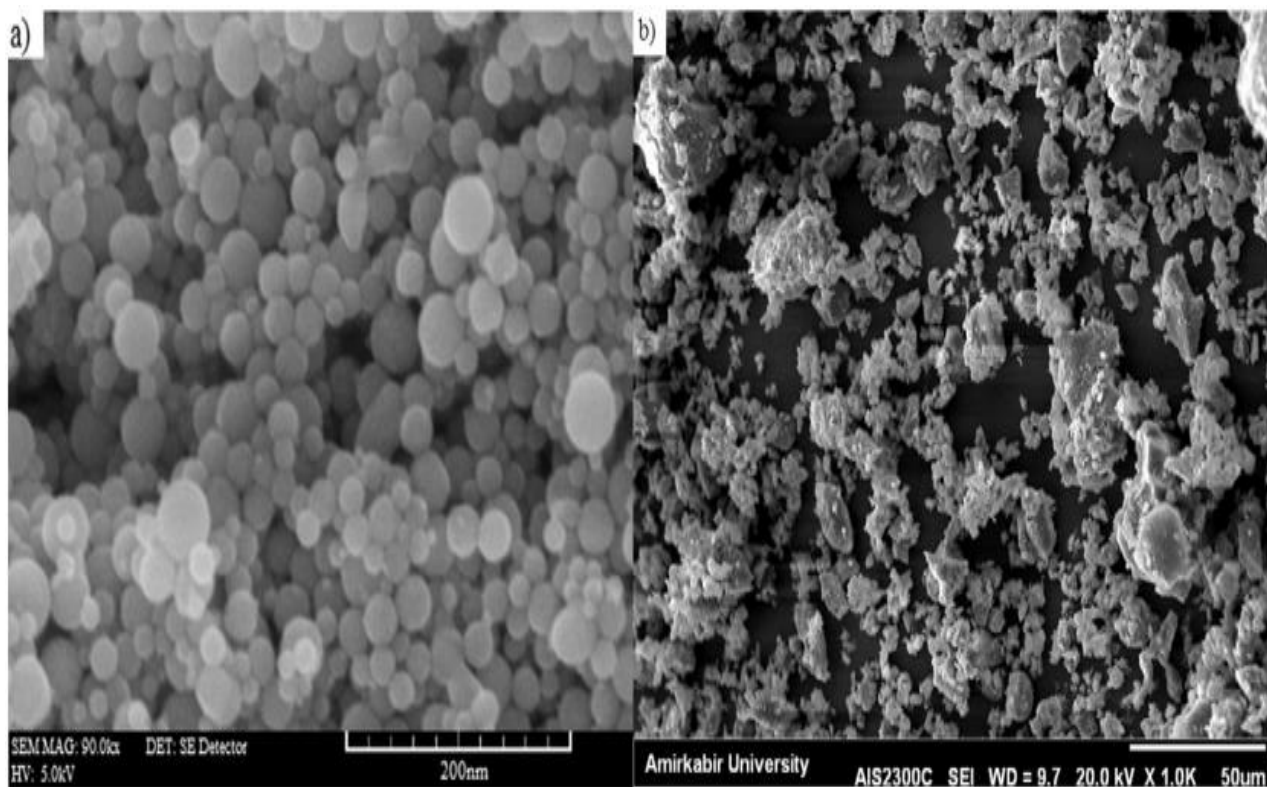


**Figure 1. (a) SEM images of NA (b) SEM images of RHA particles [24]**

## Colloidal Silica

(Anet *et al.*, 2020) explored phase composition, colloidal silica (NS), reactivity, and microstructure development of silica gel to identify a suitable system. The findings indicated that at high temperatures, the silica gel's phase composition was only marginally influenced by the environment and carbon [25]. (Lu *et al.*, 2021) discussed the rheological behavior of newly created cement-based porous materials (CPMs), and then went on to talk about dry density of silica sol, pore structure, thermal conductivity, compressive strength, and the process of pore-forming CPMs. [26]. (Tabuchi *et al.*, 2022) have invented nickel-aluminum-zirconium complex hydroxide (NAZ) with NS as binder to create a granulated agent for attracting contaminants from water based solutions by small, medium and large samples with various particle sizes were generated to assess an impact on characteristics. The materials were granulated with a 25% binder content. A SEM picture of the prepared samples is presented in Figure 2. The three groups of particles with the smallest diameters were NAZ-S, NAZ-M, and NAZ-L. [27]. (Sikora *et al.*, 2020) explored the impact of NS and 1, 3, and 5 weight percentages of saline on cement made with Portland cement slurry moisture, strengthening, and microstructural features [28].

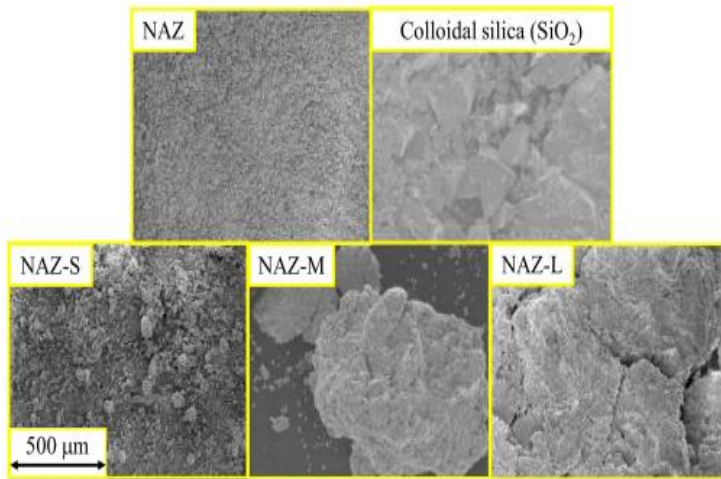


**Figure 2. SEM images of prepared absorbents [27]**

### Cement Composite

(Bhatta *et al.*, 2021) researched the effects of colloidal nano-silica on fresh and cured concrete properties. Various replacement dosages of colloidal nano-silica with a particle size of 40 nm were utilized in this study with a concentration of 30% [29]. (Yu *et al.*, 2020) conducted a number of experiments using fly ash/binder ratio of 50% by weight to evaluate an impact of NS on structural features and fracture of polyvinyl alcohol (PVA) fiber reinforced HVFAM. Four PVA fiber volume dosages were also employed [30]. (Liu *et al.*, 2019) offered a field study of adverse effects on autogenous shrinkage of cement-based materials using nanotubes of carbon, calcium carbonate, and nano montmorillonite. The effects of nanomaterials on cement paste were investigated by comparing various doses of carbon nanotubes, nano-montmorillonite, and nanocalcium carbonate with the reference group [31]. (Lavergne *et al.*, 2019) Analyzed how nano-silica affects cement paste hydration, rheology, and strength development. Analyses using thermogravimetric analysis and isothermal calorimetry are used to track the progress of chemical processes. Therefore, it may be feasible to modify recommended amount of nano-silica to promote the growth of early developmental endurance. By partially replacing fly ash for cement, a ternary mix may be created that significantly reduces CO<sub>2</sub> emissions without sacrificing either the short-term or long-term strength [32].

### Influence of Nano Binders on Refractory Castable

(Chen *et al.*, 2021) addressed feasibility of using MgO powder as castable binder in Hydratable Magnesium Carboxylate (HMC) compounds. The study focused on thermal shock resistance, green structural characteristics of calcium aluminate cement-bonded castables (CACC), and HMC-bonded castables (HMCC). Standing at 1.8 times CACC value, the maximum residual strength ratio is 56.8% [33]. (Madej and Tyrała., 2020) addressed the formation of Mg<sub>6</sub>Al<sub>2</sub>CO<sub>3</sub>(OH)<sub>16</sub>•4H<sub>2</sub>O, a magnesium-alumina spinel precursor and part of a nanostructured matrix for cement-free corundum-spinel refractory castables. It can lead high performance materials. The examination of the thermal degradation and production of spinel in the nano-structured matrix constitutes the exclusive focus of the work [34]. (Nath *et al.*, 2019) highlighted a simple method for producing “Al<sub>2</sub>O<sub>3</sub>-CaO-Cr<sub>2</sub>O<sub>3</sub> refractory castables”, which are utilized for reduce Cr by in-situ secondary phase alteration using simple silica sol. CaO/SiO<sub>2</sub> ratios of 1.45, 5.8, and 2.9 for basic silica sols were doped without compromising their castability [35]. (Miguel *et al.*, 2021) evaluated the addition of varying concentrations of Aluminium Hydroxyl Lactate (AHL) to caustic magnesia-bonded castables in order to prevent brucite precipitation throughout samples' curing, create refractories and drying processes that are free of cracks. The generated compositions were assessed for X-ray diffraction (XRD), thermogravimetric characteristics, porosity, setting behavior, permeability, cold flexural strength, and flowability [36].

(Chen *et al.*, 2021) examined how boric acid affected the microstructure development and mechanical characteristics of castables joined by HMC. The bulk density, mechanical strength, thermal shock resistance,

sintering performance, and apparent porosity of castables were evaluated. Figure 3 demonstrates the castables' residual strength rate. The reabsorbed intensity rate of HMCC fluctuates with increasing boric acid dosage. When 1% boric acid is applied, the rate reaches an elevation of 29.7%. The residual strength rate of HMCC is also much greater than that of CACC.[37].(Ding *et al.*, 2018)tested features of Al<sub>2</sub>O<sub>3</sub>-MgO resistant castables paired with carbon back, hybrid substances, Secar71, and in situ, CCAC, covering oxidation resistance, strengths, and resilience to corrosion [38]. (Giovannelli-Maizo *et al.*, 2019)studied novel powdered micro silica-alumina material, self-flowing high-alumina castables in conjunction with hydratable alumina, or both. Numerous techniques including hot elastic modulus, flowability testing, thermogravimetric measurements, hot and cold mechanical strength, erosion resistance, and others, were used to characterize the recommended compositions. A castables sintered more quickly with the addition of boron, performing best at temperatures of 815 °C or even 1100 °C for mixtures with only the silica-based additive [39].

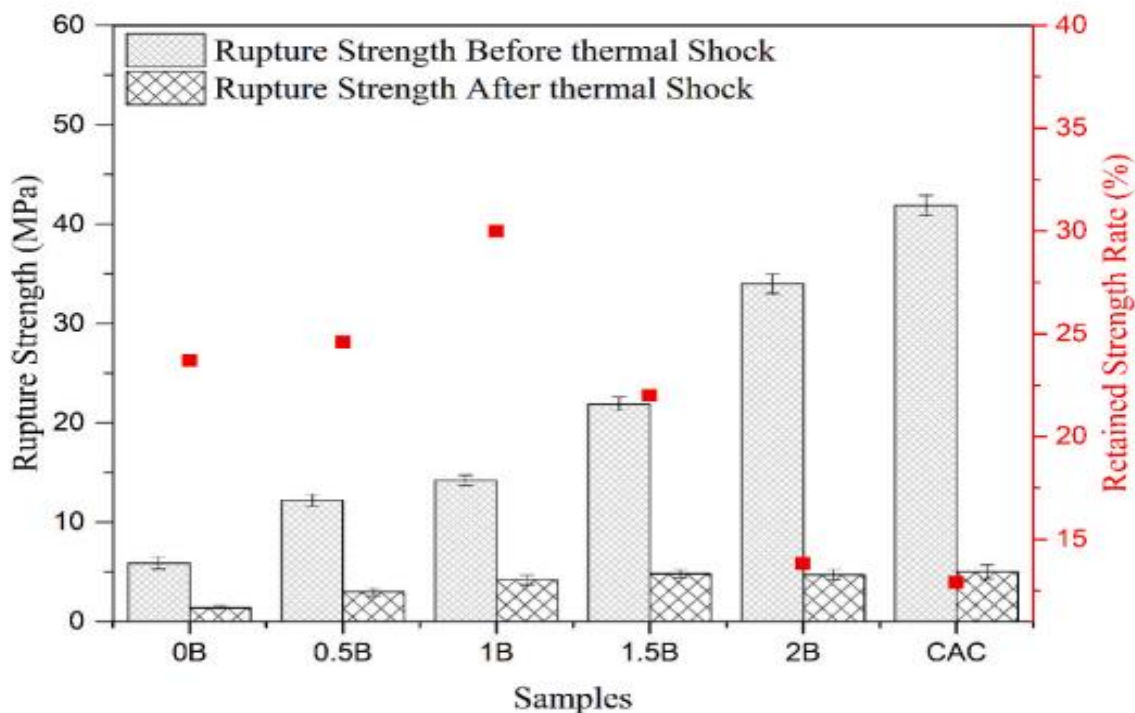


**Figure 3. The castables' residual strength rate [37]**

(Júnior and Baldo., 2019)showed a novel method for obtaining advantageous impacts on thermal and mechanical properties, backed by in-situ alumina nanoparticle production in castable matrix. After fire, an aqueous resin made using Pechini technique which produced alumina nanoparticles went through in-situ pyrolysis and oxidation [40].(Xiao *et al.*, 2018)developed in-situ CCAC through carbon-bed annealing calcium citrate tetrahydrate and Al<sub>2</sub>O<sub>3</sub> as basic components.

Infrared carbon-sulfur analysis, XRD, field-emission SEM, Raman spectroscopy, high-resolution transmission electron microscopy, and XRD were used to characterize the synthesized product. [41]. (Luz *et al.*, 2016)examined high-alumina castables containing submicron-Al<sub>2</sub>O<sub>3</sub>, SioxX®-Zero or colloidal silica using a novel alumina-silica-based powdered binders. Results showed that even though burnt SioxX®-Zero-containing castables had a high cold mechanical strength, they reduced hot modulus of rupture above 1000°C. The thermo-mechanical performance of these refractories improved when an additive that encourages transient liquid sintering was introduced during 600°C to 1200°C temperature range [42].

### High-Alumina Nano-Bonded Refractory Castables

(Hossain and Roy., 2019) presented novel binding system for unshaped refractories, namely nano-lakargiite (NL) [CaZrO<sub>3</sub>]. This formation was carried out using a simple and environmentally friendly method called solution mixing, which makes recycling the byproducts quite easy. Old eggshells serve as a supply of CaO for

making NL. Figure 4 displays an SEM micrograph of NL substrates burned in 1500 and 1600 degrees Celsius. It demonstrates that the form and size of the grains in the sintered sample at 1500 °C are irregular, ranging from 112 nm to 468 nm. On the surface, several intergranular holes have also been found [43].(Abbasian and Omidvar-Askary., 2019)studied the microstructure and phase using a field emission SEM fitted with an XRD and EDX analyzer. The production of hibonite phase in refractory is depends on temperature, and adding nano-titania might lower this temperature and increase refractory strength.The refractory castable containing nano-titania burned at 1550 °C showed a loss in cold bending strength but an increase in cold compressive strength [44].(Luz *et al.*, 2015)focused on effects of thermo-mechanical and phase formation properties of generated samples in two Al(OH)<sub>3</sub> sources added to H<sub>3</sub>PO<sub>4</sub> solutions or refractory formulations. Thermogravimetric measurements, XRD, hot elastic modulus, setting time, flowability, and mechanical efficiency were among many experimental tests that were performed [45]. (Luz *et al.*, 2018)studied significance of SioxX®-Zero and submicron alumina on rheological and structural characteristics of vibratable high-alumina castables to assess efficacy for NA floating alternatives. The metrics employed to assess the created formulations were creep tests, thermal shock resistance, hot elastic modulus, both hot and cold mechanical assets, and visible porosity in temperature range of 110°C to 1400°C[46].

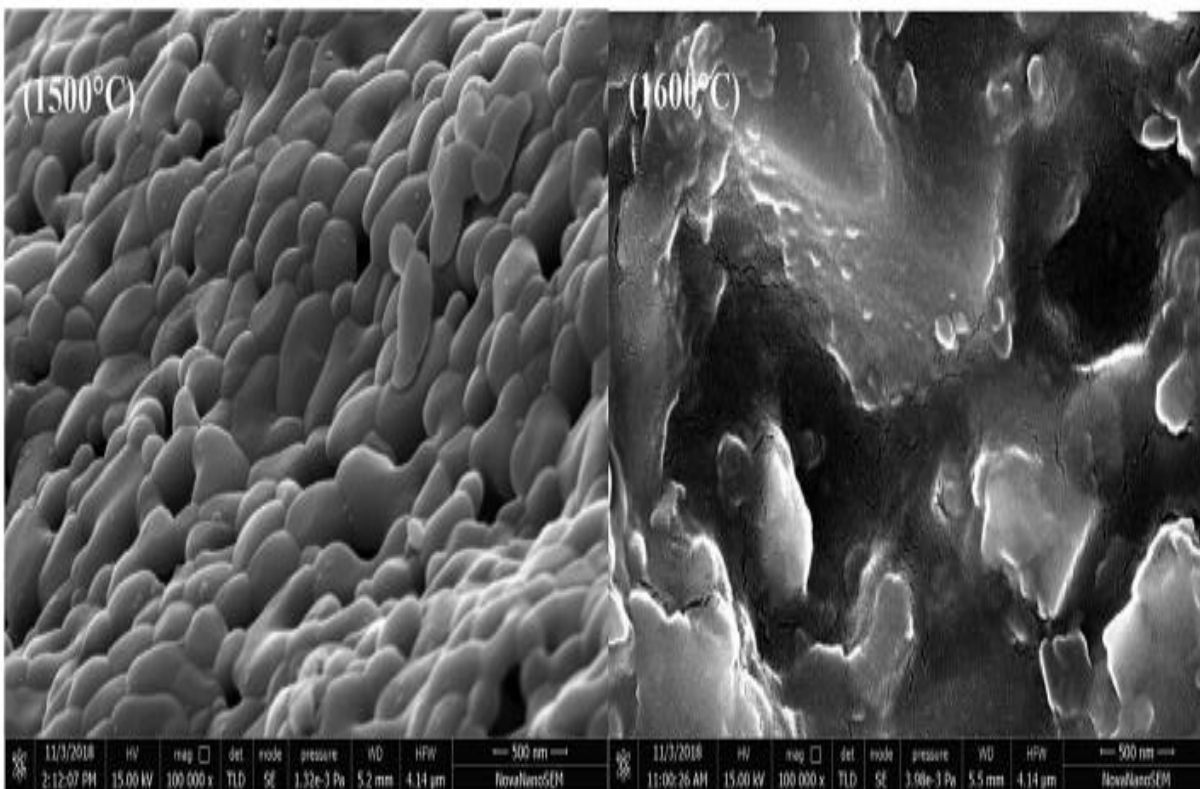


**Figure 4. SEM micrograph of sintered lakargiite surfaces at 1500°C and 1600°C [43]**

(Singh and Sarkar., 2017)evaluated several sol-gel bonding techniques for castable refractory with high alumina content.The Dinger and Funk model describes four distinct sol systems that have been separately synthesized and employed as single binders. These systems are alumina, spinel, boehmite,and mullite.

The commercial silica sol bonded formulations exhibited superior heat and corrosion capabilities, but their strength was greater because of their higher solid content [47].(Singh and Sarkar., 2018)synthesized cement-free alumina, ultra-pure castables with nano oxide bonding for high-temperature applications using several sol systems with urea as precipitating and hydrolyzing agent.

Nano-oxide powders consisting of spinel, mullite, and alumina compositions are used to connect the constables together; the matching sols serve as adhesives. The sols are employed in high alumina castable formulations and are made from nitrate precursors with urea. Figure 5 shows a percentage strength retention (in terms of numbers of thermal cycles) for the various batch compositions subjected to heat shock [48].

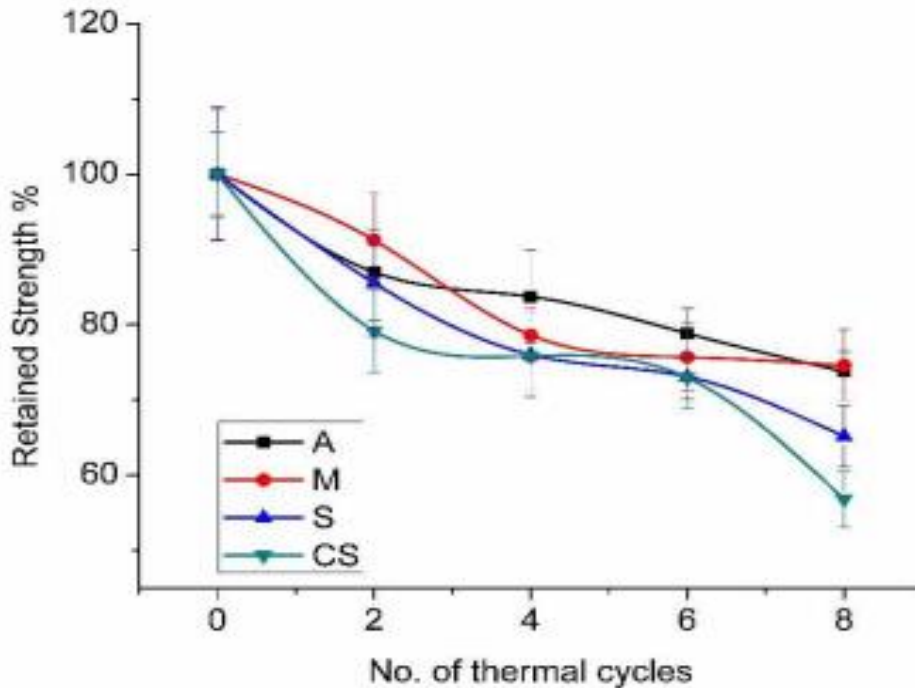


**Figure 5. Silica sol bound castables are resistant to thermal shock in batches that have been produced and contain sol [48]**

(Luz *et al.*, 2018) reviewed the use of reactive alumina and calcium aluminate cement as binders in self-reinforced high-alumina refractories. Micro silica and boron carbide were also added to several produced compositions in order to promote in-situ growth of needle-like morphological Al<sub>18</sub>B<sub>4</sub>O<sub>33</sub> or CA<sub>6</sub> phases [49]. (Pinto *et al.*, 2020) examined the potential of several additives to optimize Al<sub>2</sub>O<sub>3</sub>-MgO castables' drying behavior. After adding Polymeric Fibers, organic salt, SiO<sub>2</sub>-based additives, or permeability-enhancing active compounds (MP) to dry mixes, vibratable compositions were evaluated [50].

(Lopes *et al.*, 2017) focused on creating high-alumina self-flowing castables that are set using magnesium oxide (MgO) as a setting agent and bonded with either H<sub>3</sub>PO<sub>4</sub> solution or a combination of MAP and phosphoric acid solutions [51]. (Luz *et al.*, 2018) focused on creation of high-alumina castables that are vibratory and contain either powdered MAP or liquid MAP as binding agents. The obtained results show that both of the additives that were evaluated are very effective. Additionally, they have the benefit of not raising a temperature of castables during the mixing and curing processes unlike mixtures made with phosphoric acid. This mixture performed better overall than some of the commercial products [52].

### Sintering Additives on Castable Behavior

(Vargas *et al.*, 2021) intended to determine the fracture energy of mullite-zirconia aggregates in a high-alumina refractory at 600°C. The material's fracture energy rose by almost 30% at a 50°C rise in sintering temperature, and it is greater at 600°C than in room temperature testing [53].

(Maizo *et al.*, 2017) examined the effects of adding minerals to oxide based castable mixtures that were fused using hydrated silica at weight percentages of 0.5, 1.0, and 2.0. Boron oxide, sodium borosilicate, boric acid, magnesium borate, and boron carbide are among the materials [54]. (Luz *et al.*, 2018) concentrated on using in situ techniques such as hot elastic modulus, aided sintering and other conventional methods like thermal shock resistance, mechanical strength, etc. to evaluate compositions incorporating calcium aluminate cement, or CaCO<sub>3</sub>, or their blend. At intermediate temperatures, this method also improved the specified refractories' tensile strength and resistance to thermal shock [55].

(Yuan *et al.*, 2018) studied the influences of coarse responsive aluminium granules on characteristics of magnesium and silica castables treated with  $\text{TiO}_2$ . SEM and XRD were used to study the structure of the phases and morphology of castables including various amounts of  $\text{TiO}_2$  and two fine reactive alumina fines [56]. (Hou *et al.*, 2019) examined the sintering property of the refractory using synthesized magnesia-alumina spinel precursor sol as binder and fused magnesia as matrix. The impact of spinel precursor sol on sintering characteristics of fused magnesia refractory was examined following heat treatment at temperatures of 1450 and 1550 degrees Celsius [57].

(Yu *et al.*, 2018) evaluated the impact of sintering temperature on physical and microstructural development of in situ-produced  $\text{Si}_3\text{N}_4$  bonded  $\text{MgO-C}$  refractory. The obtained findings were indicated that  $\text{Si-N}_2$  reaction of  $\text{MgO-C}$  refractories in 1450°C produced  $\text{Si}_3\text{N}_4$ . CSS drops between 1550 °C and 1600 °C due to loss of gaseous components and making many holes in specimens [58].

(Wu *et al.*, 2020) raised features in  $\text{Al}_2\text{O}_3$  poly hollow microsphere ceramics by actually attaching  $\text{CaSiO}_3$  to surface of  $\text{Al}_2\text{O}_3$  PHMs by the use of co-precipitation strategy. The compressive strength of  $\text{Al}_2\text{O}_3$  PHM ceramics increased as their porosity decreased. The pores between  $\text{Al}_2\text{O}_3$  PHMs and the interior hollow spaces of  $\text{Al}_2\text{O}_3$  PHMs make up the majority of very high porosity of  $\text{Al}_2\text{O}_3$  PHM ceramics as illustrated in Figure. 6 [59]. (Kang *et al.*, 2019) investigated influence of  $\text{TiO}_2$  additive's dissolution on titanium melts and the sintering behavior of Y-doped  $\text{BaZrO}_3$ . To address the challenge of Y-doped  $\text{BaZrO}_3$  sintering performance, 0–5 weight percent  $\text{TiO}_2$  was added, and its densification was examined using a density analyzer, SEM, and XRD [60].

(Stortiet *et al.*, 2022) developed a straightforward method for electrospinning titanium dioxide precursor fibers. Raman spectroscopy was used to examine crystalline structure. Fibers were not dispersed uniformly throughout mixing process which might account for subpar performance seen in castables containing electrospun fibers [61].

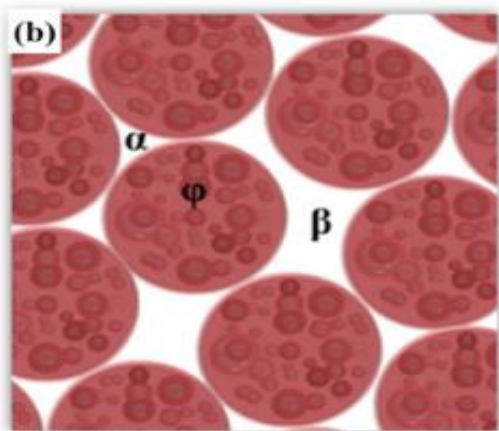


**Figure 6. Schematic representation of many types of pores found in  $\text{Al}_2\text{O}_3$  PHM ceramics.**

(Tang *et al.*, 2021) examined the possibility of using chromium to speed up process of creating forsterite ceramics from iron oxide sludge via radio smelting residue and adding sintered magnesia and chromium oxide ( $\text{Cr}_2\text{O}_3$ ) in amounts ranging from 0 to 10 weight percent. It was found to have a compressive strength of 197 MPa, a bulk density of 2.97 g/cm<sup>3</sup>, an apparent porosity of 1.4%, and a thermal shock resistance of six times. Figure 7 shows that, as compared to traditional sintering, the refractory materials produced by microwave sintering have superior thermal shock resistance (TSR) [62]. (Khalil *et al.*, 2019) Added varying amounts of nano zirconia powder (2, 4, 6, 8, and 10 weight percent) to refractory bricks made of 50% kaolin and 50% alumina increased their physico-mechanical and refractory characteristics. Aluminosilicate bricks were made with bauxite and raw kaolin. To create nano zirconia ( $\text{ZrO}_2$ ) powder, zirconium oxy chloride ( $\text{ZrOCl}_2$ ) and ammonia solution ( $\text{NH}_4\text{OH}$ ) were utilized [63]. (Gómez-Rodríguez *et al.*, 2019) proposed to assess the effects of adding  $\text{ZrO}_2$  nanoparticles (1, 3, and 5 weight percent) to bricks made of magnesia. Nanoparticles of  $\text{ZrO}_2$  generated through freezing isostatic compression and sintering at 1650 degrees Celsius were found in 5% of sample with lowest porosity and highest resistance to blast furnace slag penetration [64]. (Stonys *et al.*, 2021) went through the effects of hollow

corundum microspheres (HCM) on behavior of thermal shock resistance and physical-mechanical characteristics in refractory medium cement castable with bauxite aggregate. [65].

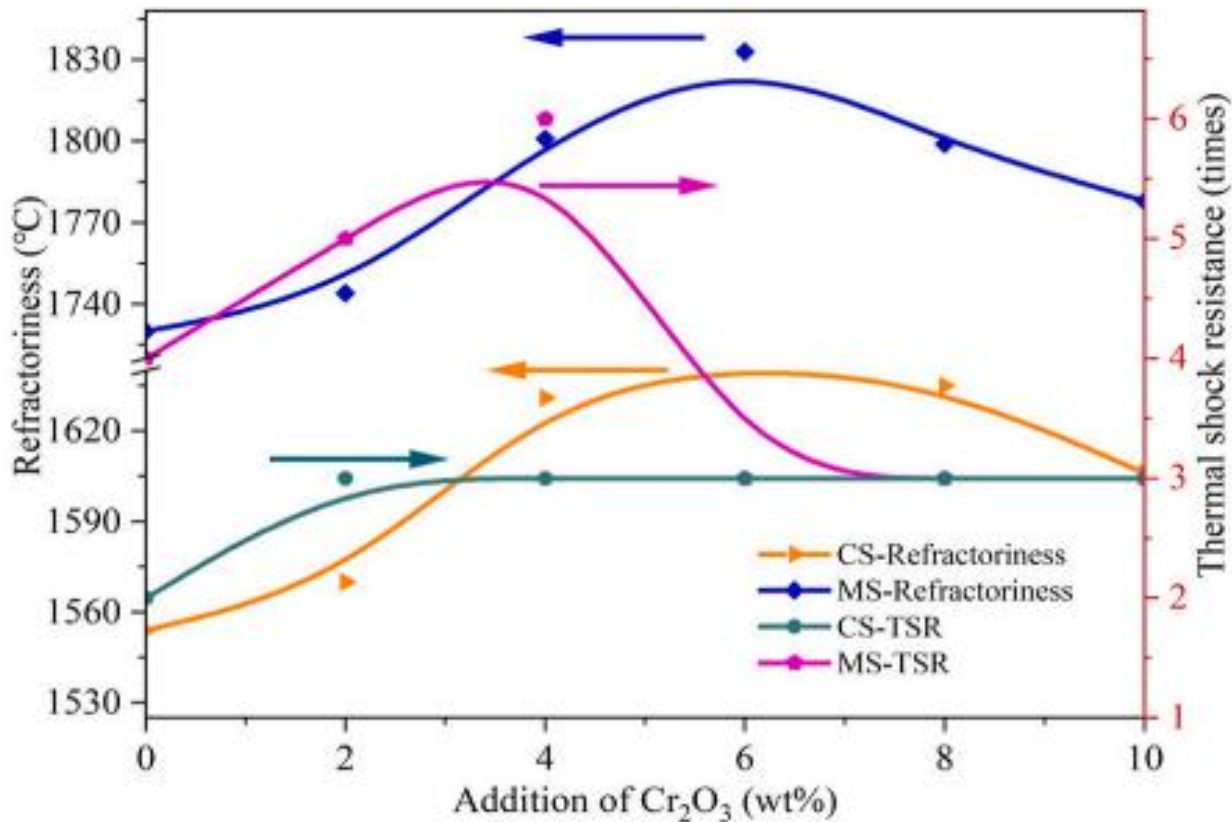


**Figure 7.impact of Cr<sub>2</sub>O<sub>3</sub> addition on thermal shock resistance and refractoriness of refractory materials made using microwave and traditional sintering techniques [62]**

### Combined Influence of Nano Binders and Sintering Additives

(Li *et al.*, 2019) discovered the specific structure and compositional organization in TiB<sub>2</sub>–5 weight proportion HEAs copper with mapping assessment from an energy dispersive spectrophotometer (EDS) and transmission electron microscopy (TEM). The capacity for flexion has substantially increased. HRTEM images confirm evidence of a supra nano dual phase structure in the as-sintered concrete adhesive, delivering the binder component to nearly its full strength [66]. (Kozekananet *al.*, 2022)analyzed the phase analysis and thermodynamics of SiC-Nano composites generated using pressure-free smelting, taken into account varying secondary phase weight percentages of 0, 0.5, 1, and 2 wt%[67]. (Oh *et al.*, 2019)established a two-stage master cremation trajectory concept following evaluating the thermal characteristics of nano, tiny, and nanotechnology/micro-bimodal particles. Three bimodal powder samples, as well as micro and nano sampleswere produced using powder injection moulding.

The samples' microstructures were studied at various sintering temperaturesand a dilatometer was used to sinter the samples and monitor the densification behavior [68].(Belyakov., 2020) explained the many ceramic sintering techniques that may be used to create high-density, pore-free ceramics.It has been demonstrated that the formation of strong aggregates (local compaction) is impossible at various phases of the production process for ceramic preparation. The usage of two-component binders, the major component being up to 20 vol.% of binder, and the second component serving as support, seems promising [69].(Chao *et al.*, 2023)used TiN-Ti-AlN as binder, PCBN elements that include and exclude Y<sub>2</sub>O<sub>3</sub> have been made at exceedingly. The chemical layout, interfacial crack anatomy, and substructure of mixture were examined with XRD and SEM. The XRD patterns of PCBN samples sintered at 1500°C with varying Y<sub>2</sub>O<sub>3</sub> are displayed in Figure. 8[70].

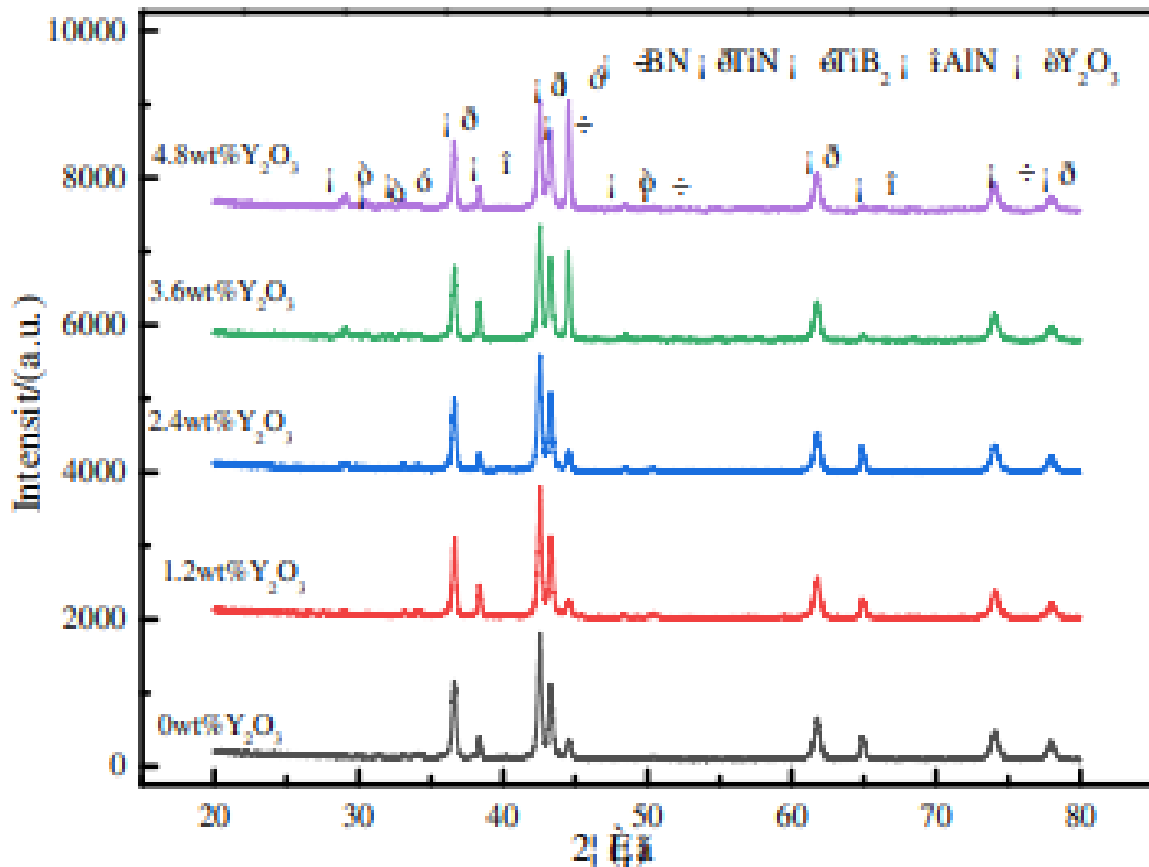


**Figure 8.**PCBN samples subjected to different  $Y_2O_3$  sintering temperatures at  $1500^\circ C$  were analyzed employing XRD.

(Wang *et al.*, 2020) created NiFe<sub>2</sub>O<sub>4</sub>/nano-TiN ceramics using a two-step cold-pressing sintering procedure. Investigations were done on mechanical performance, high-temperature conductivity, fracture morphology, and sintering behavior [71]. (Lvet *et al.*, 2020) The samples were subjected to SPS in  $1350^\circ C$  and 50 MPa to create novel WC-Ni hard metals with varying addition quantities of ZrC nano powder.

The effects of adding this were investigated on mechanical properties of samples as well as the microstructure characteristics by use of thorough characterizations using physical property, SEM, and XRD measurements. [72]. (Ji *et al.*, 2019) synthesized cBN composite by utilizing Al<sub>2</sub>O<sub>3</sub>, Si<sub>3</sub>N<sub>4</sub>, and Al as the primary binders during High Temperature High Pressure (HTHP) sintering. An extensive analysis was conducted to determine how Y<sub>2</sub>O<sub>3</sub> addition affected the mechanical and thermal characteristics of cBN composites.

The findings demonstrate that the addition of Y<sub>2</sub>O<sub>3</sub> to composites during HTHP sintering process resulted in production of eutectic melt Y-Si-Al-O-N, and suggested the eutectic liquid's volume and appearance hastened up decomposition of material composites[73]. (Zawrah *et al.*, 2020) enhanced the kaolin-based geopolymer's characteristics by optimizing the effective proportion of nano sand.

Alkali-activated kaolin-based geopolymers were supplemented with several weight percentages of nano sand, namely 2.5, 5, and 7.5 wt-%. The improvements in microstructure, compressive strength, and physical features of sintered and non-sintered geopolymer was seen upon addition of 2.5% nano sand. [74].

(Ryu *et al.*, 2019) examined the use of vacuum stretching and heating in conjunction with intense pulsed light (IPL) sintering to create warpage-free printed electronics circuits. Cu NP/MP-ink was utilized since earlier research shown that, as a result of better packing density, IPL sintered Cu NP/MP-ink displayed reduced resistivity when compared to Cu NP-ink alone [75]. (Weng *et al.*, 2020) described the use of low-temperature

microwave-assisted sintering at 1250°C to improving hardness and microstructural characteristics of three Mol percentage Yttria Stabilized Zirconia (3Y-TZP) ceramics with TiO<sub>2</sub> granules added.

The starting powders used in this experiment were 94.3% pure 3Y-TZP powders. Particle size range of 300 nm to 600 nm, 99.85% pure nano-TiO<sub>2</sub> powders were used as doping material [76]. (Pukas *et al.*, 2020) examined how the primary technical component, WC concentration, and sintering temperature affected TiC-xWC-5VC-18NiCr alloys' phase composition as shown by X-ray phase analysis.

The NaCl-type quaternary phase and solid solution of Cr were discovered to be predominant phases in alloys under investigation [77]. (Tanget *et al.*, 2020) suggested Low-concentration in-situ polymer binders were sprayed onto pieces using thermal-bubble inkjet technology.

A technique for blending fine powder was employed to improve the mechanical characteristics and capillary force of powder bed [78]. (Kwiatkowski *et al.*, 2023) presented the findings from a comparison of five different Al<sub>2</sub>O<sub>3</sub> ceramic powder grades. CT3000SG, CL370, CT1200SG, A16SG, and CT530SG are the five types of Al<sub>2</sub>O<sub>3</sub> powders used in this study. The outcomes demonstrated that from beginning of Al<sub>2</sub>O<sub>3</sub> particleless melting process, particle size, specific surface area, and width of their dispersion had a substantial impact. [79].

### Testing on refractory castables

(Vargas *et al.*, 2022) developed Wedge Splitting Test (WST) to determine the extent to which testing and sintering temperatures impact cohesive characteristics of an alumina refractory comprising mullite-zirconia aggregates. Four of the five tests that were analyzed were conducted at 600°C [80]. (Pan *et al.*, 2020) recommended utilizing WST and Digital Image Correlation (DIC) technology to examine fracture behavior of pre-treating temperatures, cement-bonded corundum castables, and different cement contents.

The castables shows maximum load and highest fracture energy at 1600°C with a cement concentration of 10% because the right amount of CA<sub>6</sub> is used [81].

(Vargas *et al.*, 2021) proposed a method that may be used in situations when Crack Mouth Opening Displacement (CMOD) is not available to estimate the fracture energy using Notch Opening Displacement (NOD) data. Finite element models and DIC are used to determine NODs and CMODs for both faces of two WST conducted on castable refractory [82].

(Czechowski *et al.*, 2015) intended to ascertain the impact of testing parameters on the testing outcomes that are connected to CCS determination process. The factorial layout and variance modeling approaches were used for identifying experimental events that had most significance on CCS estimation in scenario of thickly emerged, thermally efficient, and unshaped elements [83]. (Xu *et al.*, 2021) examined the impact of graphite concentration on fracture patterns of magnesium oxide-calcium refractories during WST using DIC and Acoustic Emission (AE) technologies.

Higher graphite content MgO-C refractories were expected to produce cracks earlier in the loading process and to have bigger final crack mouth opening displacement.

Using steel clamp, eight AE sensors with frequency bandwidth between 50 and 400KHz were positioned symmetrically on the specimen's front and rear surfaces for the experiment, as seen in Figure 9 [84]. (Haines *et al.*, 2022) determined the mixture of water and solid components with particles smaller than 0.5 mm make up the "matrix." Experimental mixtures were produced using a volume percent approach to accommodate variations in specific gravities of constituent parts.

This method fixes the percentage of water in the volume and gives you the option to swap out any solid ingredients with an equivalent volume of different refractory materials [85].

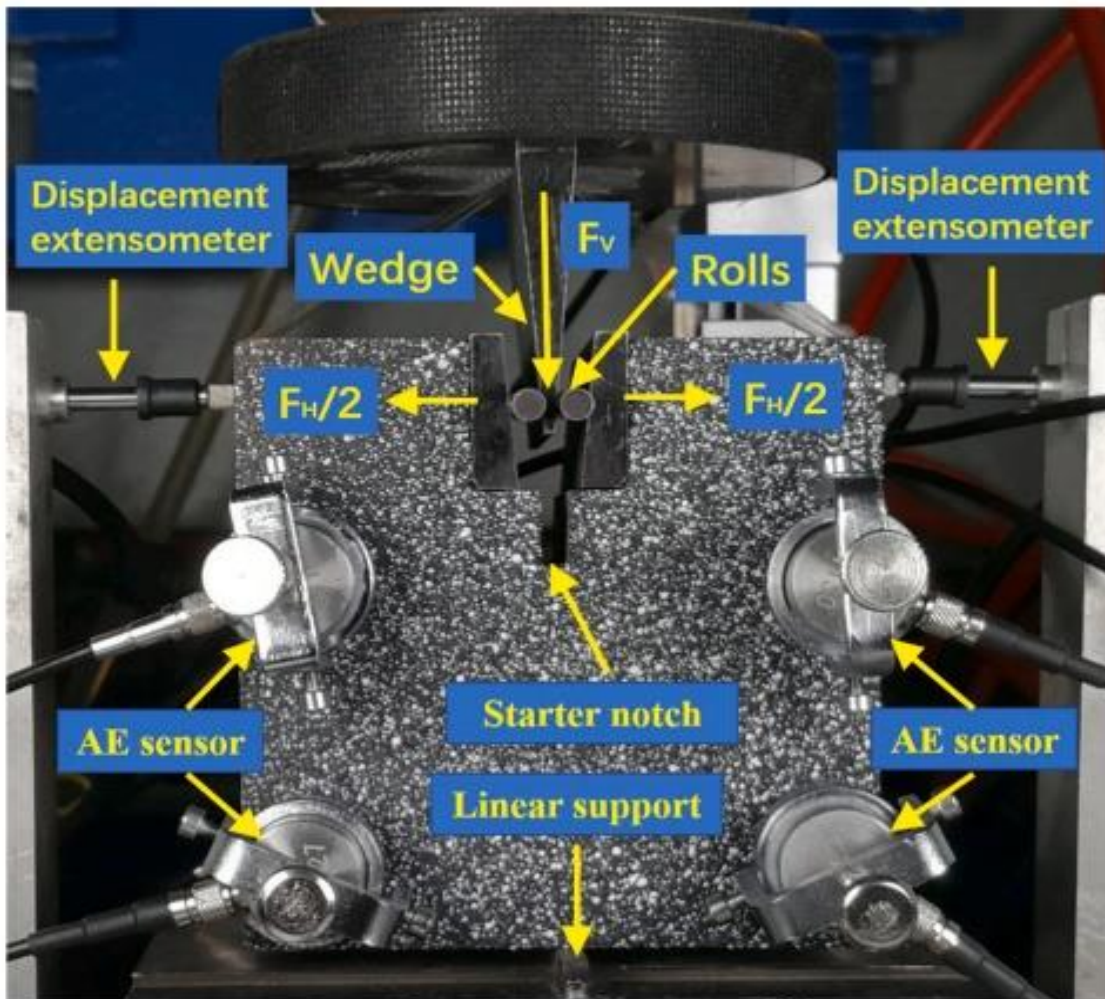


**Figure 9. Wedge Splitting Test setup in an experimental setting with DIC and AE monitoring [84]**

(Andreev *et al.*, 2019) described several approaches for evaluating thermal shock in refractories. Two traditional silica bricks and two novel fused silica materials were examined for their thermal shock capabilities. Techniques such as cyclic strain-controlled fatigue testing, repeated thermal shock tests, and fracture mechanical tests with monotonic loading have been used [86]. (Dai *et al.*, 2017) investigated how microstructure affects the way that magnesia refractories fracture.

The quasi-brittle materials were subjected to WST, which allows stable crack propagation to ascertain fracture behavior and evaluate energy dissipation. During entire cycle of WST, the fracture lengths of magnesia and spinel materials are measured based on localized strain measured with DIC [87]. (Vargas *et al.*, 2021) described a recommended procedure for calibrating these fracture characteristics utilizing force information from WST and NOD obtained using DIC. The material and boundary condition parameters were calibrated within same framework using weighted finite element modelling [88]. (Mammar *et al.*, 2016) suggested the use of a high-temperature tensile testing apparatus to evaluate creep over an extended period of time under operational loads.

The selected specimen shape is more suited for evaluating common ceramic refractories, which might vary in terms of chemical composition and maximum grain size (e.g., 5 mm) [89]. (Dai *et al.*, 2019) examined chrome-containing magnesium-spinel, tensile failure of magnesium, rebound magnesium-chrome, and refractories using Brazilian test. In order to examine the fracture process and validate validity of Brazilian test, AE and DIC were applied simultaneously [90].

(Darban *et al.*, 2022) studied the commercial alumina-spinel refractory's corrosion mechanism between 1350 and 1450 degrees Celsius. The structure and morphology changes after corrosion refractory was investigated using

XRD and EDS techniques, respectively. Corrosion produced new phases, including gehlenite, calcium hexaluminate, and calcium dealuminate [91].

(Zemánek and Nevřivová *et al.*, 2022) demonstrated how the internal structure of the material and corrosion resistance is affected by the concentration of sol particles and the distribution of pore sizes. Sol-gel castables exhibit superior corrosion resistance compared to ultra-low cement castables, according to an examination of transition zone between corrosive medium and tested castables [92]. (Zhu *et al.*, 2017) examined the fracture behavior of low carbon MgO–C refractories with various carbon sources and used WST and microscopic fractographic analysis to estimate the refractories' thermal shock resistance compared to sample where carbon source was flaky graphite [93].

(Modarresifar *et al.*, 2016) determined the most precise and reliable technique for measuring the thermal conductivity of fiber-type insulation materials, and look into the reasons for measurement variability. In order to minimize transformation, a refractory reference material that can survive test temperatures up to 1673 K was devised.

There has been some proven heterogeneity in the recorded thermal conductivities across various test techniques, such as thermal diffusivity by laser flash, hot wire, and ASTM and BS panel calorimeters [94]. (Belrhiti *et al.*, 2015) designed to compare a magnesia spinel sample to a pure magnesia sample using DIC during WST in order to examine effect of spinel addition on fracture behavior [95].

### Research Gap and Challenges

This part of the article covers the research gap in the area of types of nano binders, refractory castables, high alumina nano bonded castables, sintering additives, combination of both additives and binders, and various testing of methods of castables. It identifies the materials used in each field, benefits, and drawbacks. Table 1 shows the types of binders used in nano technology such as cement, nano alumina, and silica. Also, their outcomes are displayed along with it.

Table 2 illustrates the influence of various nano binders used in refractory castables. It also shows materials used in it and identifies their advantages and limitations.

Table 3 indicates the various high alumina nano bonded refractory castables along with their benefits and drawbacks. Table 4 demonstrate the various sintering additives which are in practice currently along with limitations. Table 5 displays existing combination of sintering additives on bonders with advantages and disadvantages. Table 6 illustrate the various existing testing methods used for refractory castables.

**Table 1:** Various types of existing nano binders

Ref	Author & year	Aim	Types	Outcomes
[21]	Younus <i>et al.</i> 2023	To examine implications of introducing NA on mobility, mechanical features, and passing efficiency of an FA-based A-ASCC that experienced external curing.	nano-alumina	The maximum compressive and flexural strengths were attained.

[22]	Su <i>et al</i> 2020	To research the structural consequences of various nano-alumina additions.	nano-alumina	Under this criteria, complete mechanical characteristics are best.
[23]	Shao <i>et al</i> 2019	To understand the fundamental mechanisms and explain how NA affects longterm mechanical properties of cementbased materials.	nano-alumina	NA dissolves slowly, and its disintegration is gradual.
[24]	Mohseni <i>et al.</i> , 2019	To evaluate the structural and mechanical characteristics of light geopolymers reinforced with polypropylene fibers.	nano-alumina	significant influence on flexural strength as opposed to compressive strength
[25]	An <i>et al.</i> 2020	To find suitable system for colloidal silica application	Colloidal silica	Findings demonstrated that during heating, silica gel's phase composition was somewhat influenced by carbon and the environment.
[26]	Lu <i>et al.</i> 2021	To research and report the thermal conductivity and compressive strength of CPMs.	Colloidal silica	The CPMs have a lower heat conductivity than other typical porous cement-based materials.
[27]	Tabuchi <i>et al</i> 2022	To create a granulated water purification agent by zirconium complex hydroxides, aluminium, and mixing nickel with binder.	Colloidal silica	The produced NAZ samples have a potential to be used as VI ion adsorption-desorption agents in aqueous solutions.
[28]	Sikora <i>et al.</i> 2020	To examine beneficial impacts of saltwater and commercially available NS on creation of durable cement-based composites.	Colloidal silica	The combination of saltwater and NS made it possible to create cement paste with a total porosity that was 41% lower than that of the reference DW0 specimen.

[29]	Bhatta <i>et al.</i> 2021	To examine how colloidal nanosilica affects the characteristics of fresh and cured concrete.	Cement Composite	The optimized replacement dose performed best in terms of achieving a denser and more consistent microstructure in specimen.
[30]	Yu <i>et al.</i> , 2020	To determine the influence of NS on fracture and mechanical parameters of 50% fixed HVFAM fly ash/binder ratio reinforced with PVA fiber.	Cement Composite	Insights into the fabrication and use of high-volume pozzolan cement-based composites augmented with fibers and nanoparticles.
[31]	Liu <i>et al.</i> 2019	To assess the impact of nanomaterials on cement paste, several doses of nano calcium carbonate and nano montmorillonite were examined.	Cement Composite	The first 72 hours are when cement-based materials with nanomaterials experience the majority of their autogenous shrinkage.
[32]	Lavergne <i>et al.</i>	To analyze the impact of NS on rheology, hydration, and strength development of cement pastes.	Cement Composite	The nano-silica dose may be adjusted to increase early age strength.

**Table 2:** Nano binders with various existing bonding material

Ref	Author & year	Aim	Bonded material	Advantages	Disadvantages
[33]	Chen <i>et al</i> 2021	To examine the potential of MgO powder and HMC as a castables binder.	HMC	It is possible to enhance persistent linear change during thermal shock resistance.	A linear crack is formed
[34]	Madej and Tyrała 2020	To research the synthesis and thermal behavior of $Mg_6Al_2CO_3(OH)_{16} \cdot 4H_2O$ as a component of nano-structured matrix and magnesia-alumina spinel precursor for cement-free corundum-spinel refractory castables.	Mg–Al layered double hydroxide-like phases formed within the nano-MgO–nano-Al <sub>2</sub> O <sub>3</sub> blended paste	High performance material. Increased crystallinity with increased processing temperature	The study is limited to the analysis of the thermal decomposition and formation of spinel in the nano-structured matrix

[35]	Nath <i>et al</i> 2019	To create Al <sub>2</sub> O <sub>3</sub> - CaO- Cr <sub>2</sub> O <sub>3</sub> refractory castables system using common silica, a simple method has been used.	basic silica sol (pH~9)	Substantially easier after-use disposal or recycling and substantially smaller Cr waste generation	At 1500°C, just a few faint peaks (CA6) could be seen.
[36]	Miguel <i>et al</i> 2021	To prevent cracks in produced samples' refractories by managing the brucite precipitation during drying and curing processes.	Aluminum Hydroxyl Lactate	There were no visible fractures or refractory structural damage.	
[37]	Chen <i>et al</i> 2021	To study the consequences of fatty acids on microstructural development and mechanical attributes of castables attached to HMC.	Boric acid	Improve the thermal shock resistance. Increased bonding strength.	After the thermal shock, microcracks are larger and wavier.
[38]	Ding <i>et al</i> . 2018	To find out the features of castables bound with Secar71, CCAC, and S71CB which consist of Al <sub>2</sub> O <sub>3</sub> -MgO.	in situ CCAC	Improved resistance to rusting. Enhanced resistance to oxidation	There is no limitation is discussed in this paper.
[39]	Giovannelli- Maizo <i>et al</i> 2019	To evaluate calcium-free binders bonded at 4 weight percent for self-flowing high-alumina castables	calcium-free binders	Erosion resistance. Thermal shock resistance.	Thermal expansion mismatch among generated phases.

[40]	Júnior and Baldo 2019	To achieve beneficial impacts on the mechanical and thermal characteristics	85 wt% Al <sub>2</sub> O <sub>3</sub>	Flexural strength. Elastic modulus.	No drawbacks are discussed
[41]	Xiao et al 2018	To synthesize In-situ CCAC via carbon-bed sintering with calcium citrate tetrahydrate and Al <sub>2</sub> O <sub>3</sub> as raw materials	in-situ calcium aluminate cement with carbon	Higher strength. Better water dispersion.	Easily oxidized
[42]	Luz et al 2016	To evaluate submicron Al <sub>2</sub> O <sub>3</sub> , SiOX®-Zero, or colloidal silica castables with high alumina.	Silica-Based and Alumina Binders	Lower elastic modulus. Thermal shock resistance reduced.	Limitations are not specified.

**Table 3:** Comparison of various existing high alumina nano bonded castables

Ref	Author & year	Aim	Binder used	Advantages	Disadvantages
[43]	Hossain and Roy 2019	To supply nano-lakargiite (NL) [CaZrO <sub>3</sub> ], a novel binder system, for unshaped refractories	nano-lakargiite	There are financial and ecological benefits.	Not specified
[44]	Abbasian and Omidvar-Askary 2019	To look into how adding nano-titania to high alumina castables affects their mechanical and microstructural properties.	nano-titania	Thermal shock resistance is decreased. Enhances mechanical strength.	Decreased cold bending strength.

[45]	Luz et al 2015	To evaluate the phase development effects of two Al(OH) <sub>3</sub> sources included in H <sub>3</sub> PO <sub>4</sub> solutions or refractory formulations	Al(OH) <sub>3</sub> and H <sub>3</sub> PO <sub>4</sub>	<ul style="list-style-type: none"> <li>Improved hot and cold mechanical performance.</li> <li>Higher elastic modulus and mechanical strength.</li> </ul>	There is no drawbacks were discussed.
[46]	Luz et al 2018	To discover if they may serve as viable substitutes for colloidal silica suspensions.	Alumina-silica-based powdered binders	<ul style="list-style-type: none"> <li>Good flowability level.</li> <li>Higher thermal stability.</li> </ul>	HMOR values decrease at 1000°C.
[47]	Singh and Sarkar 2017	To compare several sol-gel bonding methods for castable refractory with high alumina content.	alumina, boehmite, mullite, and spinel	<ul style="list-style-type: none"> <li>High strength.</li> <li>Improved thermos mechanical and corrosion resistance</li> </ul>	Not specified
[48]	Singh and Sarkar 2018	To mix and match with urea serving as both the precipitating and hydrolyzing agent, cement-free, high-purity alumina castables.	Nano- oxide	<ul style="list-style-type: none"> <li>Corrosion resistance is high.</li> <li>Improved shock resistance.</li> </ul>	Reduced corroding activity.

[49]	Luz et al 2018	To examine the assessment of high-alumina self-reinforced refractories that use calcium aluminate cement and reactive aluminas as binders.	AloxX spheres and/or submicron alumina	High thermal stability. Enhanced Thermo mechanical behavior.	These samples still contained a significant amount of liquid at a high temperature.
[50]	Pinto <i>et al</i> 2020	To look into the potential of different additives to improve drying behavior of castable Al <sub>2</sub> O <sub>3</sub> -MgO.	MgO	High explosion resistance. Increases mechanical strength.	samples breaking at 110°C when drying. Enhanced slag penetration.
[51]	Lopes et al 2017	To generate self-flowing castables with high alumina content that are bonded using either H <sub>3</sub> PO <sub>4</sub> solution or a combination of MAP and phosphoric acid solutions.	H <sub>3</sub> PO <sub>4</sub>	Higher green mechanical strength.	This substance did not give the compositions bound with H <sub>3</sub> PO <sub>4</sub> an adequate working period.
[52]	Luz et al 2018	To focuses on the construction of vibratable high-alumina castables with binding agents such as magnesium monophosphate powder or MAP (liquid).	MAP (liquid) or magnesium monophosphate (powder)	Overall performance is better. Easy to handle and prepare.	Not specified.

**Table 4:** Comparison of existing sintering additives

Ref	Author & year	Aim	Material used	Advantages	Disadvantages
[53]	Vargas <i>et al</i> 2021	To calculate fracture energy of 12-high-alumina refractory at 600°C that contains aggregates of zirconia and mullite.	Alumina-Mullite-Zirconia	Higher propensity for initiating cracks.	Displacement fluctuations were higher due to heat haze.
[54]	Maizo et al 2017	To determine the contribution of five distinct SA added at 0.5, 1.0, and 2.0 weight percent to castable compositions	B <sub>2</sub> O <sub>3</sub> , H <sub>3</sub> BO <sub>3</sub> , BS, BM, B <sub>4</sub> C.	Faster sintering. Enhanced thermo chemical performance.	All the evaluated compositions did not show full transient liquid phase sintering.

		based on alumina and bonded with hydratable alumina.			
[55]	Luz <i>et al.</i> 2018	To look into how long CA6 grains are formed and calcium carbonate plays a part in that process.	calcium carbonate	Improved resilience to thermal shock and mechanical strength.	Poor binding after drying at 110°C for 24 hours and curing at 50°C
[56]	Yuan <i>et al.</i> 2018	To evaluate certain reactive alumina powders with varying amounts of impurities, such as Na <sub>2</sub> O and SiO <sub>2</sub> .	alumina-magnesia castables with TiO <sub>2</sub>	Higher cold moduli of rupture.	Reactive alumina affected on phase evolution.
[57]	Hou <i>et al.</i> 2019	To examine the sintering properties of fused magnesia refractory using synthesized magnesia-alumina spinel precursor sol as binder and fused magnesia as matrix.	magnesia-alumina spinel precursor sol	increased linear shrinkage while adding precursor sol at the same time	The excessive spinel precursor volume expansion that occurred during the heating phase.
[58]	Yu <i>et al.</i> 2018	To determine whether the temperature during sintering affects the shape and physical characteristics of the Si <sub>3</sub> N <sub>4</sub> -bonded MgO-C refractory that is produced in situ.	Si <sub>3</sub> N <sub>4</sub> -bonded MgO-C	Great strength. improve the overall physical properties of refractories.	Reduces the bearing capacity of specimen.

[59]	Wu <i>et al</i> 2020	To improve the properties of Al <sub>2</sub> O <sub>3</sub> poly-hollow microsphere ceramics.	Al <sub>2</sub> O <sub>3</sub> PHM ceramics.	Compressive strength increases. Sintering necks became stronger.	Porosity decreases.
[60]	Kang <i>et al</i> 2019	To investigate sintering behavior of Y-doped BaZrO <sub>3</sub> with TiO <sub>2</sub> additive and effects of its dissolution on titanium melts.	Y-doped BaZrO <sub>3</sub> with TiO <sub>2</sub> .	Better erosion resistance.	No limitations are discussed
[61]	Storti <i>et al</i> 2022	To assess the impact of these fibers on low-cement, high-alumina castables in comparison to commercial polypropylene fibers (PP).	Tabular alumina, calcium aluminate binder.	Highest final permeability.	uneven distribution of fibers during mixing process
[62]	Tang <i>et al</i> 2021	To research the chromium-assisted microwave sintering process for preparing forsterite refractory materials from ferronickel slag.	ferronickel slag, sintered magnesia and chromium oxide.	There was a six-fold increase in thermal shock resistance, and 197 MPa compressive strength.	Not specified
[63]	Khalil <i>et al</i> 2019	To evaluate the mechanical, refractory, and densification factors.	kaolin and bauxite, ZrOCl <sub>2</sub> and NH <sub>4</sub> OH	The superior densification properties of this sample are responsible for its exceptional performance.	There are no disadvantages were specified.

[64]	Gómez-Rodríguez <i>et al</i>	To determine the effects of adding ZrO <sub>2</sub> nanoparticles to bricks made of magnesia.	ZrO <sub>2</sub> , MgO	Lowest porosity and greatest resistance	No limitations
[65]	Stonys <i>et al</i> 2021	To investigate the impact of HCM on behaviour of thermal shock resistance and the physical and mechanical characteristics of refractory medium cement castable with bauxite aggregate.	High alumina cement Gorkal, Reactive alumina, Bauxite, Calcined alumina	Increasing Thermal resistance, Reduces stress concentration in regular shape.	Increase in stress concentration of irregular shape.

**Table 5:** Comparison of various existing combined nano binders and sintering

Ref	Author & year	Aim	Materials used	Advantages	Disadvantages
[66]	Li <i>et al</i> 2019	To concentrate on precise shape and elemental distribution using TEM and EDS mapping investigation in TiB <sub>2</sub> -5 weight percent HEAs ceramic.	TiB <sub>2</sub> powder, HEAs cermet.	The binder has perfect strength and outstanding wetness.	This scenario is unsuitable to grain boundary sliding hypothesis.
[67]	Kozekanan <i>et al</i> 2022	To examine SiC-nano/microB <sub>4</sub> C composites' thermodynamic and phase analysis	SiC-nano/micro B <sub>4</sub> C	Raises intensity at its climax. Increases graphitization level.	If added wt%- Resin Phenolic is removed, sintering process is not finished.

[68]	Oh <i>et al</i> 2019	To investigate thermal sintering characteristics of materials that are micro, nano, and nano/micro-bimodal.	Fe NP and MP, KMC-21	high density and small grains. High accuracy.	Their multi-peak shrinking behaviors resulted in significant errors.
[69]	Belyakov 2020	To explain several ceramic sintering techniques that enable the creation of high-density, pore-free ceramics.	Micro- and Nano-Grain Size Ceramics	high density. Prevents crystal growth.	Not discussed
[70]	Chao <i>et al</i> 2023	To employ TiN-Ti-AlN as binder to create PCBN composites with and without Y <sub>2</sub> O <sub>3</sub> .	TiN-Ti-AlN, XRD, SEM.	Improved sintering performance. Best comprehensive mechanical properties	This process requires more energy.
[71]	Wang <i>et al</i> 2021	To prepare NiFe <sub>2</sub> O <sub>4</sub> /nano-TiN ceramic samples in an argon environment using a two-step cold-pressing sintering procedure.	NiFe <sub>2</sub> O <sub>4</sub> /nano-TiN	High temperature conductivity. Reduces sintering temperature	Not mentioned any limitation.
[72]	Lv <i>et al</i> 2020	To use XRD, SEM, and measurements of physical characteristics to look into effects of ZrC nanopowder on microstructure and mechanical properties.	ZrC, WC, Ni	Maximum relative density.	The specimens' predicted flexural strength continuously declined.

[73]	Ji <i>et al</i> 2019	To create cBN composite utilizing Si <sub>3</sub> N <sub>4</sub> , Al <sub>2</sub> O <sub>3</sub> , and Al as the primary binders by HTHP sintering	Al <sub>2</sub> O <sub>3</sub> , Si <sub>3</sub> N <sub>4</sub> , and Al	High relative density. High bending strength.	High oxidation temperature.
[74]	Zawrah <i>et al</i> 2020	To enhance the kaolin-based geopolymer's characteristics by optimizing the effective proportion of nano sand.	Liquid sodium silicate, NaOH	Improved compressive strength.	Decrease in the efficiency of geopolymerization.
[75]	Ryu <i>et al</i> 2019	To research vacuum stretching and heating of polymer substrate during IPL sintering process.	Cu NP/MP-ink	Improved packing density. Low resistivity.	There is no limitations were mentioned.
[76]	Weng <i>et al</i> 2020	To investigate the impact on 3Y-TZP's phase, hardness, and grain size of addition of nano TiO <sub>2</sub> particles.	3Y-TZP, TiO <sub>2</sub>	Sintered at low temperature	Not described.
[77]	Pukas <i>et al</i> 2020	To look for how WC concentration and sintering temperature affect phase composition.	TiC-xWC-5VC-18NiCr alloys.	Better intensity.	A W <sub>2</sub> C phase was not detected.
[78]	Tang <i>et al</i> 2020	To print Ti6Al4V parts through jetting minimum concentration in-situ polymer binders thermal-bubble using inkjet technology.	Ti6Al4V	Higher density.	Complicated lightweight structure.
[79]	Kwiatkowski <i>et al</i> 2023	To enhance the process for powder bed fusion technology material selection for 3D printing.	Five types of Al <sub>2</sub> O <sub>3</sub> powders (A16SG, CT3000SG, CT1200SG, CT530SG, and CL370)	Possible to control the quality of the printout.	No Drawbacks were mentioned.

**Table 6:** Comparison of various test methods used for refractory castables

Ref	Author & year	Aim	Method	Advantages	Disadvantages
[80]	Vargas <i>et al</i> 2022	To evaluate the cohesive qualities of aggregates made of mullite and zirconia in an alumina refractory.	wedge splitting tests (WST)	scatter of cohesive parameters is desirable	Damage initiating at half the ultimate load.
[81]	Pan <i>et al</i> 2020	To look at how cement-bonded corundum castables fracture.	WST and digital image correlation (DIC) technique	By adding more cement, such castables' brittleness can be decreased.	Highest extent of crack propagation within the matrix
[82]	Vargas <i>et al</i> 2021	To explore correlations between CMOD and NOD through numerical simulations.	WST, DIC	Crack propagation energy can easily be estimated	Crack initiation is more complex.
[83]	Czechowski <i>et al</i> 2015	To ascertain the impact of testing settings on the CCS determination process	Cold Crushing Strength (CCS)	CCS value was found to be higher at a higher load rate	Negative effect of packing.
[84]	Xu <i>et al</i> 2021	To investigate the impact of graphite content on MgO-C refractory fracture behavior.	WST, DIC, Acoustic Emission (AE)	A higher graphite content improved the resistance to further fracture propagation.	Energy dissipation and the nonlinear mechanical behaviour of loading process

[85]	Haines <i>et al</i> 2022	To measure alkali phases' depth of penetration into the refractory crucible and to ascertain the post-test corrosive phases that developed.	Pre-test microstructural analysis and XRD analysis	To generate mullite and liquid phases and aid in decreasing porosity in the final product.	The refractory's campaign life is obviously impacted by the increased porosity.
[86]	Andreev <i>et al</i> 2019	To explain several approaches for evaluating thermal shock in refractories.	XRF and XRD	High strain tolerance and low brittleness that promotes resistance to crack growth and thermal shock	Not discussed
[87]	Dai <i>et al</i> 2017	To study the impact of microstructure on magnesia refractory fracture behavior.	WST, DIC	Even in situations when the strength drops, curved crack route and formation of FPZ raise specific fracture energy.	Not mentioned.
[88]	Vargas <i>et al</i> 2021	To offer a manual for calibrating these fracture characteristics using NOD.	WST, DIC	excellent agreement between grey level residual fields, NOD, displacement, and splitting force.	The Young's modulus had larger deviations.
[89]	Mammar <i>et al</i> 2016	To suggest the use of high-temperature tensile testing apparatus that enables long-term creep assessments under working loads.	finite element (FE) model	Achieved uniform loading avoided bending stresses.	There is no discussion on creep mechanisms or creep parameter modifications.
[90]	Dai <i>et al</i> 2019	To explore the tensile failure of magnesium, rebound magnesium-chrome, and magnesium-spinel including chrome refractories.	Brazilian test, AE, DIC	The brittleness reduction enables a quasi-stable crack propagation	lower strength for larger volume.

[91]	Darban <i>et al</i> 2022	To investigate the process for industrial alumina-spinel refractory corrosion at temperatures of 1350 °C and 1450°C.	SEM/EDS and XRD	The production of new calcium aluminate layers is covered within indirect absorption of alumina.	Not discussed
[92]	Zemánek and Nevřivová <i>et al</i> 2022	To study internal structure of material and corrosion resistance is affected by concentration of sol particles	WDXRF,	Increased resistance to corrosion for a sol-gel castable	No drawbacks were discussed.
[93]	Zhu <i>et al</i> 2017	To assess thermal shock resistance quantitatively	WST, microscopic fractographic analysis	Increases thermal shock resistance, fracture energy, and characteristic length.	Inversely connected to elastic modulus
[94]	Modarresifar <i>et al</i> 2016	To determine the best accurate and repeatable technique for measuring thermal conductivity	BS panel calorimeters, hot wire, and ASTM	Good mechanical strength	Not mentioned.
[95]	Belrhiti <i>et al</i> 2015	To study the influence of spinel addition on fracture behavior	WST, DIC	Mechanical properties dependent on their microstructure.	High level of damage induced by micro-cracks

## CONCLUSION

This research provides significant illumination on how the mechanical features, microstructures, and fresh and hardened properties of cementitious and ceramic materials are affected by nano alumina, nano silica, and other nanomaterials. It was investigated how the addition of NA impacts microstructure and functionality of A-ASCC and how it interacts with various binders. The investigation of colloidal silica, phase composition, encompassing its microstructure, and reactivity provides essential insights for the advancement of silica gel-based systems,

especially for high-temperature applications. Future research and development in this sector can benefit greatly from the potential and challenges found in these investigations. In order to satisfy the changing needs of refractory applications, these studies investigate the use of various binders, additives, and processes to improve chemical mechanical, and thermal characteristics of castables. The field of refractory materials and larger industrial sectors they service will be greatly impacted by the cumulative insights provided by this research. In the fields of refractory castables and high-performance materials, the results of these investigations together provide a multitude of insights and advances. They include information on cutting-edge processes, additives, and binder systems that may be used for create refractory substances with enhanced characteristics and performance.

The area of castables and refractory materials has greatly progressed as a result of the varied and creative research reported in these works. The results show that high-performance, sustainable, and eco-friendly refractory solutions may be developed and adapted to a variety of industrial uses. These discoveries advance the continuous development of refractory materials, opening the door to improved functionality, adaptability, and robustness under demanding operating circumstances. Additionally, this review offers important new understandings of the mechanisms controlling the sintering process and the alterations in refractory material performance and microstructure that follow. The combined results further our knowledge of how these additives might be strategically used to modify the characteristics of refractories for certain uses. The research results enhance the continuous progress of refractory technology by providing avenues for customizing materials for particular uses and refining their performance attributes. By using this abundance of information, scientists and engineers may create refractories that are highly reliable and long-lasting, meeting the rigorous demands of many industries and operating environments.

The importance of sintering additives and nano binders in modifying the characteristics of different materials, such as composites and ceramics, is highlighted by all of this study taken together. Their discoveries aid in the creation of high-performance materials for a variety of uses, including structural elements and electronics. A greater knowledge of phase composition and microstructural changes both essential for material design and optimization has been made possible by advanced characterization techniques. The refractory castable investigations that are discussed in the text include information about thermal shock resistance, mechanical behavior, and microstructural features of refractory particles. The study advances creation of refractory materials with better qualities which are essential for use in sectors with harsh working environments and high-temperature operations. It also emphasizes the significance of precise characterization and testing methodologies in the assessment of refractory materials.

## ACKNOWLEDGMENT

The authors would like to express their sincere gratitude to SERB for financial assistance and the Central Instrument Facility Centre (CIFIC) at IIT (BHU), Varanasi for technical support. The authors also extend heartfelt thanks to the Department of Ceramic Engineering at IIT (BHU), Varanasi, for valuable suggestions throughout the research work.

## REFERENCES

1. Otitoju, T.A., Okoye, P.U., Chen, G., Li, Y., Okoye, M.O. and Li, S., 2020. Advanced ceramic components: Materials, fabrication, and applications. *Journal of industrial and engineering chemistry*, 85, pp.34-65.
2. Oses, C., Toher, C. and Curtarolo, S., 2020. High-entropy ceramics. *Nature Reviews Materials*, 5(4), pp.295-309.
3. Mohajerani, A., Burnett, L., Smith, J.V., Kurmus, H., Milas, J., Arulrajah, A., Horpibulsuk, S. and Abdul Kadir, A., 2019. Nanoparticles in construction materials and other applications, and implications of nanoparticle use. *Materials*, 12(19), p.3052.

4. Alas, M., Ali, S.I.A., Abdulhadi, Y. and Abba, S.I., 2020. Experimental evaluation and modeling of polymer nanocomposite modified asphalt binder using ANN and ANFIS. *Journal of Materials in Civil Engineering*, 32(10), p.04020305.
5. Karnati, S.R., Oldham, D., Fini, E.H. and Zhang, L., 2019. Surface functionalization of silica nanoparticles to enhance aging resistance of asphalt binder. *Construction and building materials*, 211, pp.1065-1072.
6. Nesor, B., Chromkova, I., Szklorzova, H., Prachar, V., Svitak, O., Stanek, L. and Nejedlik, M., 2022, September. A new approach for the determination of thermal shock resistance of refractories. In *Journal of Physics: Conference Series* (Vol. 2341, No. 1, p. 012006). IOP Publishing.
7. Ouyang, J.H., Li, Y.F., Zhang, Y.Z., Wang, Y.M. and Wang, Y.J., 2022. High-temperature solid lubricants and self-lubricating composites: A critical review. *Lubricants*, 10(8), p.177.
8. Eze, V.H.U., Uche, C.K.A., Chinyere, U., Wisdom, O. and Chukwudi, O.F., 2023. Utilization of Crumbs from Discarded Rubber Tyres as Coarse Aggregate in Concrete: A Review. *International Journal of Recent Technology and Applied Science (IJORTAS)*, 5(2), pp.74-80.
9. Bai, P., Etim, U.J., Yan, Z., Mintova, S., Zhang, Z., Zhong, Z. and Gao, X., 2019. Fluid catalytic cracking technology: current status and recent discoveries on catalyst contamination. *Catalysis Reviews*, 61(3), pp.333-405.
10. Schuler, E., Demetriou, M., Shiju, N.R. and Gruter, G.J.M., 2021. Towards sustainable oxalic acid from CO<sub>2</sub> and biomass. *ChemSusChem*, 14(18), pp.3636-3664.
11. Velázquez, H.D., Cerón-Camacho, R., Mosqueira-Mondragón, M.L., Hernández-Cortez, J.G., Montoya de la Fuente, J.A., Hernández-Pichardo, M.L., Beltrán-Oviedo, T.A. and Martínez-Palou, R., 2023. Recent progress on catalyst technologies for high quality gasoline production. *Catalysis Reviews*, 65(4), pp.1079-1299.
12. Jagtiani, E., 2022. Advancements in nanotechnology for food science and industry. *Food Frontiers*, 3(1), pp.56-82.
13. Butt, O.M., Bibi, S., Ahmad, M.S., Che, H.S., Zahid, T., Bibi, S. and Abd Rahim, N., 2022. Hydrogen as Potential Primary Energy Fuel for Municipal Solid Waste Incineration for a Sustainable Waste Management. *IEEE Access*, 10, pp.114586-114596.
14. Bembenek, M., Popadyuk, O., Shihab, T., Ropyak, L., Uhryński, A., Vytvytskyi, V. and Bulbuk, O., 2022. Optimization of technological parameters of the process of forming therapeutic biopolymer nanofilled films. *Nanomaterials*, 12(14), p.2413.
15. Deutou, J.G.N., Kaze, R.C., Kamseu, E. and Sglavo, V.M., 2021. Controlling the thermal stability of kyanite-based refractory geopolymers. *Materials*, 14(11), p.2903.
16. Bahaaddini, M., Baharvandi, H.R., Ehsani, N., Khajehzadeh, M. and Tamadon, A., 2019. Pressureless sintering of LPS-SiC (SiC-Al<sub>2</sub>O<sub>3</sub>-Y<sub>2</sub>O<sub>3</sub>) composite in presence of the B<sub>4</sub>C additive. *Ceramics International*, 45(10), pp.13536-13545.
17. Zhang, H. and Akhtar, F., 2020. Effect of SiC on microstructure, phase evolution, and mechanical properties of spark-plasma-sintered high-entropy ceramic composite. *Ceramics*, 3(3), pp.359-371.
18. Khan, S., Allu, A.R., Gaddam, A., Fernandes, H.R., Dutta, S., Kongar, P.S., Tarafder, A., Ferreira, J.M. and Annapurna, K., 2022. Use of colemanite and borax penta-hydrate in soda lime silicate glass melting- A strategy to reduce energy consumption and improve glass properties. *Ceramics International*, 48(1), pp.1181-1190.
19. Ouyang, J.H., Li, Y.F., Zhang, Y.Z., Wang, Y.M. and Wang, Y.J., 2022. High-temperature solid lubricants and self-lubricating composites: A critical review. *Lubricants*, 10(8), p.177.
20. Kane, K.A., Pint, B.A., Mitchell, D. and Haynes, J.A., 2021. Oxidation of ultrahigh temperature ceramics: kinetics, mechanisms, and applications. *Journal of the European Ceramic Society*, 41(13), pp.6130-6150.
21. Younus, S.J., Mosaberpanah, M.A. and Alzebaree, R., 2023. The performance of alkali-activated self-compacting concrete with and without nano-Alumina. *Sustainability*, 15(3), p.2811.
22. Su, W., Zou, J. and Sun, L., 2020. Effects of nano-alumina on mechanical properties and wear resistance of WC-8Co cemented carbide by spark plasma sintering. *International Journal of Refractory Metals and Hard Materials*, 92, p.105337.

23. Shao, Q., Zheng, K., Zhou, X., Zhou, J. and Zeng, X., 2019. Enhancement of nano-alumina on long-term strength of Portland cement and the relation to its influences on compositional and microstructural aspects. *Cement and Concrete Composites*, 98, pp.39-48.
24. Mohseni, E., Kazemi, M.J., Koushkbaghi, M., Zehtab, B. and Behforouz, B., 2019. Evaluation of mechanical and durability properties of fiber-reinforced lightweight geopolymer composites based on rice husk ash and nano-alumina. *Construction and Building Materials*, 209, pp.532-540.
25. An, J., Wang, Y., Jia, Q., Zhao, F. and Liu, X., 2020. Microstructure and reactivity evolution of colloidal silica binder in different systems at elevated temperatures. *Ceramics International*, 46(12), pp.20129-20137.
26. Lu, J., Jiang, J., Lu, Z., Li, J. and Shi, Y., 2021. Preparation and properties of nanopore-rich cement-based porous materials based on colloidal silica sol. *Construction and Building Materials*, 299, p.123966.
27. Tabuchi, A., Ogata, F., Uematsu, Y., Toda, M., Otani, M., Saenjum, C., Nakamura, T. and Kawasaki, N., 2022. Granulation of Nickel–Aluminum–Zirconium Complex Hydroxide Using Colloidal Silica for Adsorption of Chromium (VI) Ions from the Liquid Phase. *Molecules*, 27(8), p.2392.
28. Sikora, P., Cendrowski, K., Abd Elrahman, M., Chung, S.Y., Mijowska, E. and Stephan, D., 2020. The effects of seawater on the hydration, microstructure and strength development of Portland cement pastes incorporating colloidal silica. *Applied Nanoscience*, 10(8), pp.2627-2638.
29. Bhatta, D.P., Singla, S. and Garg, R., 2021. Microstructural and strength parameters of Nano-SiO<sub>2</sub> based cement composites. *Materials today: proceedings*, 46, pp.6743-6747.
30. Yu, J., Zhang, M., Li, G., Meng, J. and Leung, C.K., 2020. Using nano-silica to improve mechanical and fracture properties of fiber-reinforced high-volume fly ash cement mortar. *Construction and Building Materials*, 239, p.117853.
31. Liu, X., Fang, T. and Zuo, J., 2019. Effect of nano-materials on autogenous shrinkage properties of cement based materials. *Symmetry*, 11(9), p.1144.
32. Lavergne, F., Belhadi, R., Carriat, J. and Fraj, A.B., 2019. Effect of nano-silica particles on the hydration, the rheology and the strength development of a blended cement paste. *Cement and Concrete Composites*, 95, pp.42-55.
33. Chen, J., Xiao, G., Ding, D., Zang, Y., Lei, C., Luo, J., Chong, X. and Ren, Y., 2021. Thermal shock resistance properties of refractory castables bonded with a CaO-free binder. *Ceramics International*, 47(3), pp.4238-4248.
34. Madej, D. and Tyrała, K., 2020. In situ spinel formation in a smart nano-structured matrix for no-cement refractory castables. *Materials*, 13(6), p.1403.
35. Nath, M., Song, S., Xu, T., Wu, Y. and Li, Y., 2019. Effective inhibition of Cr (VI) in the Al<sub>2</sub>O<sub>3</sub>-CaO-Cr<sub>2</sub>O<sub>3</sub> refractory castables system through silica gel assisted in-situ secondary phase tuning. *Journal of cleaner production*, 233, pp.1038-1046.
36. Miguel, V.C., Fini, D.S., Pinto, V.S., Moreira, M.H., Pandolfelli, V.C. and Luz, A.P., 2021. Crack-free caustic magnesite-bonded refractory castables. *Ceramics International*, 47(12), pp.17255-17261.
37. Chen, J., Xiao, G., Ding, D., Zhang, S., Lei, C., Zang, Y. and Ren, Y., 2021. Mechanical properties of refractory castables bonded with hydratable magnesium carboxylate-boric acid. *Ceramics International*, 47(15), pp.21221-21230.
38. Ding, D., Yang, S., Xiao, G., Ren, Y., Lv, L., Yang, P., Hou, X. and Gao, J., 2018. Investigations on the properties of Al<sub>2</sub>O<sub>3</sub>-MgO refractory castables bonded by in situ carbon containing calcium aluminate cement. *Materials Research Express*, 5(9), p.095205.
39. Giovannelli-Maizo, I.D., Luz, A.P. and Pandolfelli, V.C., 2019. Advanced boron-containing refractory castables bonded with calcium-free binders. *Ceramics International*, 45(7), pp.8774-8782.
40. Júnior, J.A.A. and Baldo, J.B., 2019. The Effect of Nano-Alumina Particles Generated in Situ in the Matrix of Ultralow and No Cement 85 wt% Al<sub>2</sub>O<sub>3</sub> Refractory Castables. *Journal of Materials Science and Chemical Engineering*, 7(6), pp.7-22.
41. Xiao, G., Yang, S., Ding, D., Ren, Y., Lv, L., Yang, P., Hou, X. and Gao, J., 2018. One-step synthesis of in-situ carbon-containing calcium aluminate cement as binders for refractory castables. *Ceramics International*, 44(13), pp.15378-15384.

42. Luz, A.P., Lopes, S., Pandolfelli, V.C. and Gomes, D.T., 2016. Advanced refractory castables containing novel alumina and silica-based binders. In *Proceedings of the Alafar Congress* (pp. 1-11).
43. Hossain, S.S. and Roy, P.K., 2019. Development of waste derived nano-lakargiite bonded high alumina refractory castable for high temperature applications. *Ceramics International*, 45(13), pp.16202-16213.
44. Abbasian, A.R. and Omidvar-Askary, N., 2019. Microstructural and mechanical investigation of high alumina refractory castables containing nano-titania. *Ceramics International*, 45(1), pp.287-298.
45. Luz, A.P., Gomes, D.T. and Pandolfelli, V.C., 2015. High-alumina phosphate-bonded refractory castables: Al (OH) 3 sources and their effects. *Ceramics International*, 41(7), pp.9041-9050.
46. Luz, A.P., Lopes, S.J.S., Gomes, D.T. and Pandolfelli, V.C., 2018. High-alumina refractory castables bonded with novel alumina-silica-based powdered binders. *Ceramics International*, 44(8), pp.9159-9167.
47. Singh, A.K. and Sarkar, R., 2017. High alumina castables: a comparison among various sol-gel bonding systems. *Journal of the Australian Ceramic Society*, 53, pp.553-567.
48. Singh, A.K. and Sarkar, R., 2018. Urea based sols as binder for nano-oxide bonded high alumina refractory castables. *Journal of Alloys and Compounds*, 758, pp.140-147.
49. Luz, A.P., Gabriel, A.H.G., Consoni, L.B., Aneziris, C.G. and Pandolfelli, V.C., 2018. Self-reinforced high-alumina refractory castables. *Ceramics International*, 44(2), pp.2364-2375.
50. Pinto, V.S., Fini, D.S., Miguel, V.C., Pandolfelli, V.C., Moreira, M.H., Venâncio, T. and Luz, A.P., 2020. Fast drying of high-alumina MgO-bonded refractory castables. *Ceramics International*, 46(8), pp.11137-11148.
51. Lopes, S.J.S., Luz, A.P., Gomes, D.T. and Pandolfelli, V.C., 2017. Self-flowing high-alumina phosphate-bonded refractory castables. *Ceramics International*, 43(8), pp.6239-6249.
52. Luz, A.P., Lopes, S.J., Gomes, D.T. and Pandolfelli, V.C., 2018. High-alumina chemically bonded refractory castables containing liquid or powdered binders. *Refractories WORLDFORUM*, 10(2), pp.68-73.
53. Vargas, R., Pinelli, X., Smaniotto, B., Hild, F. and Canto, R.B., 2021. On the effect of sintering temperature on the fracture energy of an Alumina-Mullite-Zirconia castable at 600 C. *Journal of the European Ceramic Society*, 41(7), pp.4406-4418.
54. Maizo, I.G., Luz, A.P., Pagliosa, C. and Pandolfelli, V.C., 2017. Boron sources as sintering additives for alumina-based refractory castables. *Ceramics International*, 43(13), pp.10207-10216.
55. Luz, A.P., Consoni, L.B., Pagliosa, C., Aneziris, C.G. and Pandolfelli, V.C., 2018. Sintering effect of calcium carbonate in high-alumina refractory castables. *Ceramics International*, 44(9), pp.10486-10497.
56. Yuan, W., Tang, H., Zhou, Y. and Zhang, D., 2018. Effects of fine reactive alumina powders on properties of alumina-magnesia castables with TiO<sub>2</sub> additions. *Ceramics International*, 44(5), pp.5032-5036.
57. Hou, Q., Luo, X., Xie, Z., An, D., Zhang, X. and Peng, Z., 2019. Effect of magnesia-alumina spinel precursor sol on the sintering property of fused magnesia refractory. *Ceramics International*, 45(3), pp.3459-3464.
58. Yu, C., Ding, J., Deng, C., Zhu, H. and Peng, N., 2018. The effects of sintering temperature on the morphology and physical properties of in situ Si<sub>3</sub>N<sub>4</sub> bonded MgO-C refractory. *Ceramics International*, 44(1), pp.1104-1109.
59. Wu, J.M., Li, M., Liu, S.S., Shi, Y.S., Li, C.H. and Wang, W., 2020. Preparation of porous Al<sub>2</sub>O<sub>3</sub> ceramics with enhanced properties by SLS using Al<sub>2</sub>O<sub>3</sub> poly-hollow microspheres (PHMs) coated with CaSiO<sub>3</sub> sintering additive. *Ceramics International*, 46(17), pp.26888-26894.
60. Kang, J., Chen, G., Lan, B., Zhang, R., Ali, W., Lu, X. and Li, C., 2019. Sintering behavior of Y-doped BaZrO<sub>3</sub> refractory with TiO<sub>2</sub> additive and effects of its dissolution on titanium melts. *International Journal of Applied Ceramic Technology*, 16(3), pp.1088-1097.
61. Storti, E., Himcinschi, C., Neumann, M., Hubáľková, J. and Aneziris, C.G., 2022. Electrospun fibers as drying additive in cement-bonded alumina castables. *International Journal of Applied Ceramic Technology*, 19(4), pp.2160-2171.
62. Tang, H., Peng, Z., Gu, F., Yang, L., Tian, W., Zhong, Q., Rao, M., Li, G. and Jiang, T., 2021. Chromium-promoted preparation of forsterite refractory materials from ferronickel slag by microwave sintering. *Ceramics International*, 47(8), pp.10809-10818.

63. Khalil, N.M., Algalal, Y., Saleem, Q.M., Aly, K.A. and Wahsh, M.M.S., 2019. Improved Refractory Aluminosilicate Bricks Through Nano Zirconia Additions. *Science and Technology*, 8(3), p.6.
64. Gómez-Rodríguez, C., Fernández-González, D., García-Quiñonez, L.V., Castillo-Rodríguez, G.A., Aguilar-Martínez, J.A. and Verdeja, L.F., 2019. MgO refractory doped with ZrO<sub>2</sub> nanoparticles: influence of cold isostatic and uniaxial pressing and sintering temperature in the physical and chemical properties. *Metals*, 9(12), p.1297.
65. Stonys, R., Malaiškienė, J., Škamat, J. and Antonovič, V., 2021. Effect of hollow corundum microspheres additive on physical and mechanical properties and thermal shock resistance behavior of bauxite based refractory castable. *Materials*, 14(16), p.4736.
66. Li, Y., Xu, H., Ke, B., Sun, Y., Yang, K., Ji, W., Wang, W. and Fu, Z., 2019. TEM characterization of a Supra-Nano-Dual-Phase binder phase in spark plasma sintered TiB<sub>2</sub>-5 wt% HEAs cermet. *Ceramics International*, 45(7), pp.9401-9405.
67. Kozekanan, B.S., Moradkhani, A., Baharvandi, H. and Ehsani, N., 2022. Thermodynamic and phase analysis of SiC-nano/microB<sub>4</sub>C-C composites produced by pressureless sintering method. *Journal of the Korean Ceramic Society*, 59(2), pp.180-192.
68. Oh, J.W., Seong, Y. and Park, S.J., 2019. Investigation and two-stage modeling of sintering behavior of nano/micro-bimodal powders. *Powder Technology*, 352, pp.42-52.
69. Belyakov, A.V., 2020. High-Density Micro-and Nano-Grain Size Ceramics. Transition from Open into Closed Pores. Part 3. Workpiece Sintering without External Pressure1. *Refractories and Industrial Ceramics*, 61(1), pp.40-49.
70. Chao, C., Peicheng, M., Jiarong, C., Xixi, H., Qiaofan, H., Feng, L. and Yi, W., 2023. Effect of Y<sub>2</sub>O<sub>3</sub> additive on properties of PCBN composites with TiN-Ti-AlN as binder by high temperature and high pressure sintering. *International Journal of Refractory Metals and Hard Materials*, 110, p.106009.
71. Wang, B., Du, J., Gao, S., Zhou, M., Li, E. and Li, L., 2020. Sintering Behavior and Fracture Morphology of NiFe<sub>2</sub>O<sub>4</sub>/Nano-TiN Ceramics Synthesized under Argon Atmosphere. *Journal of Materials Engineering and Performance*, 29, pp.7971-7980.
72. Lv, C., Ren, X., Wang, C. and Peng, Z., 2020. Spark plasma sintering of ultrafine WC-10Ni-ZrC hardmetals: effects of adding ZrC nano-powder. *International Journal of Applied Ceramic Technology*, 17(3), pp.932-940.
73. Ji, H., Li, Z., Sun, K. and Zhu, Y., 2019. Effect of Y<sub>2</sub>O<sub>3</sub> additive on properties of cBN composites with Si<sub>3</sub>N<sub>4</sub>-Al<sub>2</sub>O<sub>3</sub>-Al as binder by high temperature and high pressure sintering. *Ceramics International*, 45(16), pp.20478-20483.
74. Zawrah, M.F., Sawan, S.A., Khattab, R.M. and Abdel-Shafi, A.A., 2020. Effect of nano sand on the properties of metakaolin-based geopolymer: Study on its low rate sintering. *Construction and Building Materials*, 246, p.118486.
75. Ryu, C.H., Joo, S.J. and Kim, H.S., 2019. Intense pulsed light sintering of Cu nano particles/micro particles-ink assisted with heating and vacuum holding of substrate for warpage free printed electronic circuit. *Thin Solid Films*, 675, pp.23-33.
76. Weng, M.H., Lin, C.X., Huang, C.S., Tsai, C.Y. and Yang, R.Y., 2020. Improved microstructure and hardness properties of low-temperature microwave-sintered Y<sub>2</sub>O<sub>3</sub> stabilized ZrO<sub>2</sub> ceramics with additions of nano TiO<sub>2</sub> powders. *Materials*, 13(7), p.1546.
77. Pukas, S., Zinko, L., German, N., Gladyshevskii, R., Koval, I.V., Bodrova, L., Kramar, H. and Marynenko, S., 2020. Influence of the nano-WC content and Sintering Temperature on the Phase Composition of Hard Alloys in the System TiC-WC-Vc-NiCr. *Physics and Chemistry of Solid State*, 21(3), pp.496-502.
78. Tang, Y., Huang, Z., Yang, J. and Xie, Y., 2020. Enhancing the capillary force of binder-jetting printing Ti<sub>6</sub>Al<sub>4</sub>V and mechanical properties under high temperature sintering by mixing fine powder. *Metals*, 10(10), p.1354.
79. Kwiatkowski, M., Marczyk, J., Putyra, P., Kwiatkowski, M., Przybyła, S. and Hebda, M., 2023. Influence of Alumina Grade on Sintering Properties and Possible Application in Binder Jetting Additive Technology. *Materials*, 16(10), p.3853.
80. Vargas, R., Canto, R.B. and Hild, F., 2022. Cohesive properties of refractory castable at 600 C: Effect of sintering and testing temperature. *Journal of the European Ceramic Society*, 42(14), pp.6733-6749.

81. Pan, L., He, Z., Li, Y., Zhu, T., Wang, Q., Li, B., Dai, Y. and Xu, X., 2020. Investigation of fracture behavior of cement-bonded corundum castables using wedge splitting test and digital image correlation method. *Journal of the European Ceramic Society*, 40(4), pp.1728-1737.
82. Vargas, R., Canto, R.B. and Hild, F., 2021. Fracture energy evaluation of refractories in wedge splitting tests from notch opening displacements. *Journal of the European Ceramic Society*, 41(10), pp.5367-5379.
83. Czechowski, J., Gerle, A., Podworny, J. and Dahlem, E., 2015. Investigation of the testing parameters influencing the cold crushing strength testing results of refractory materials. *Refract. Worldforum*, 7, pp.105-112.
84. Xu, X., Li, Y., Dai, Y., Zhu, T., Pan, L. and Szczerba, J., 2021. Influence of graphite content on fracture behavior of MgO–C refractories based on wedge splitting test with digital image correlation method and acoustic emission. *Ceramics International*, 47(9), pp.12742-12752.
85. Haines, K., Byrd, K. and Lankard, D., 2022. Alkali resistance testing methodology and development: Focus on mullite based castables. *International Journal of Ceramic Engineering & Science*, 4(4), pp.240-248.
86. Andreev, K., Tadaion, V., Zhu, Q., Wang, W., Yin, Y. and Tonnesen, T., 2019. Thermal and mechanical cyclic tests and fracture mechanics parameters as indicators of thermal shock resistance—case study on silica refractories. *Journal of the European Ceramic Society*, 39(4), pp.1650-1659.
87. Dai, Y., Gruber, D. and Harmuth, H., 2017. Determination of the fracture behaviour of MgO-refractories using multi-cycle wedge splitting test and digital image correlation. *Journal of the European Ceramic Society*, 37(15), pp.5035-5043.
88. Vargas, R., Canto, R.B. and Hild, F., 2021. On the calibration of cohesive parameters for refractories from notch opening displacements in wedge splitting tests. *Journal of the European Ceramic Society*, 41(14), pp.7348-7361.
89. Mammari, A.S., Gruber, D., Harmuth, H. and Jin, S., 2016. Tensile creep measurements of ordinary ceramic refractories at service related loads including setup, creep law, testing and evaluation procedures. *Ceramics International*, 42(6), pp.6791-6799.
90. Dai, Y., Li, Y., Xu, X., Zhu, Q., Yan, W., Jin, S. and Harmuth, H., 2019. Fracture behaviour of magnesia refractory materials in tension with the Brazilian test. *Journal of the European Ceramic Society*, 39(16), pp.5433-5441.
91. Darban, S., Reynaert, C., Ludwig, M., Prorok, R., Jastrzębska, I. and Szczerba, J., 2022. Corrosion of Alumina-Spinel Refractory by Secondary Metallurgical Slag Using Coating Corrosion Test. *Materials*, 15(10), p.3425.
92. Zemánek, D. and Nevřivová, L., 2022. Development and Testing of Castables with Low Content of Calcium Oxide. *Materials*, 15(17), p.5918.
93. Zhu, T., Li, Y., Sang, S. and Xie, Z., 2017. Fracture behavior of low carbon MgO–C refractories using the wedge splitting test. *Journal of the European Ceramic Society*, 37(4), pp.1789-1797.
94. Modarresifar, F., Bingham, P.A. and Jubb, G.A., 2016. Thermal conductivity of refractory glass fibres: A study of materials, standards and test methods. *Journal of Thermal Analysis and Calorimetry*, 125, pp.35-44.
95. Belrhiti, Y., Pop, O., Germaneau, A., Doumalin, P., Dupré, J.C., Harmuth, H., Huger, M. and Chotard, T., 2015. Investigation of the impact of micro-cracks on fracture behavior of magnesia products using wedge splitting test and digital image correlation. *Journal of the European Ceramic Society*, 35(2), pp.823-829.